

GL-TR-89-0311

PSR Report 1864 - VOL-2

**IONOSPHERIC HEATING WITH OBLIQUE WAVES**

**Vol. 2. Applications to High-Frequency Radio Propagation**

**AD-A223 111**

R. M. Bloom  
E. C. Field, Jr.

Pacific-Sierra Research Corporation  
12340 Santa Monica Blvd.  
Los Angeles, California 90025

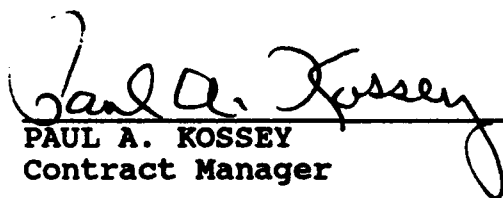
1 August 1989

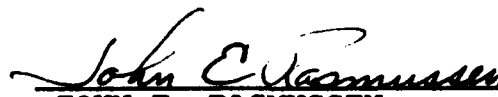
Scientific Report No. 2  
Approved for public release; distribution unlimited

Geophysics Laboratory  
Air Force Systems Command  
United States Air Force  
Hanscom Air Force Base, Massachusetts 01731-5000

**DTIC**  
**ELECTE**  
**JUN 13 1990**  
**S B D**

"This technical report has been reviewed and is approved for publication"

  
PAUL A. KOSSEY  
Contract Manager

  
JOHN E. RASMUSSEN  
Branch Chief

FOR THE COMMANDER

  
ROBERT M. SKRIVANEK  
Division Director

This report has been reviewed by the ESD Public Affairs Office (PA) and is releasable to the National Technical Information Service (NTIS).

Qualified requestors may obtain additional copies from the Defense Technical Information Center. All others should apply to the National Technical Information Service.

If your address has changed, or if you wish to be removed from the mailing list, or if the addressee is no longer employed by your organization, please notify GL/IMA, Hanscom AFB, MA 01731. This will assist us in maintaining a current mailing list.

Do not return copies of this report unless contractual obligations or notices on a specific document requires that it be returned.

## REPORT DOCUMENTATION PAGE

1a. REPORT SECURITY CLASSIFICATION UNCLASSIFIED		1b. RESTRICTIVE MARKINGS	
2a. SECURITY CLASSIFICATION AUTHORITY N/A since Unclassified		3. DISTRIBUTION/AVAILABILITY OF REPORT Approved for public release; distribution unlimited.	
2b. DECLASSIFICATION/DOWNGRADING SCHEDULE N/A since Unclassified		5. MONITORING ORGANIZATION REPORT NUMBER(S) GL-TR-89-0311	
4. PERFORMING ORGANIZATION REPORT NUMBER(S) Report 1864, Vol. 2		7a. NAME OF MONITORING ORGANIZATION Geophysics Laboratory	
6a. NAME OF PERFORMING ORGANIZATION Pacific-Sierra Research Corporation	6b. OFFICE SYMBOL (if applicable)	7b. ADDRESS (City, State, and ZIP Code) Hanscom AFB Massachusetts 01731-5000	
5c. ADDRESS (City, State, and ZIP Code) 12340 Santa Monica Boulevard Los Angeles, California 90025		9. PROCUREMENT INSTRUMENT IDENTIFICATION NUMBER F19628-87-C-0028	
8a. NAME OF FUNDING, SPONSORING ORGANIZATION Air Force Geophysics Laboratory	8b. OFFICE SYMBOL (if applicable)	10. SOURCE OF FUNDING NUMBERS	
3c. ADDRESS (City, State, and ZIP Code) Hanscom Air Force Base Massachusetts 01731		PROGRAM ELEMENT NO 61102F	PROJECT NO 2310
		TASK NO G3	WORK UNIT ACCESSION NO BL
11. TITLE (Include Security Classification) IONOSPHERIC HEATING WITH OBLIQUE WAVES; Vol. 2. Applications to High-Frequency Radio Propagation			
12. PERSONAL AUTHOR(S) Bloom, R. M., Field, E. C.			
13a. TYPE OF REPORT Scientific Report No. 2	13b. TIME COVERED FROM 870213 to 890731	14. DATE OF REPORT (Year, Month, Day) 890801	15. PAGE COUNT 46
16. SUPPLEMENTARY NOTATION			
17. COSATI CODES		18. SUBJECT TERMS (Continue on reverse if necessary and identify by block number)	
FIELD	GROUP	Ionospheric Heating High-Frequency Propagation	
	SUB-GROUP	Radio Waves	
		Electric Fields	
19. ABSTRACT (Continue on reverse if necessary and identify by block number) This volume presents numerical calculations of ionospheric electron density perturbations and ground-level signal changes for several electric field distributions produced by high-frequency (HF) transmitters. This volume applies theory developed in earlier work (Vol. 1) to the problem of possible self-effects of powerful obliquely incident radio waves. Using the results from this earlier work, we use field-driven changes in ionospheric electron density to calculate modified ambient refractive index profiles and the consequent effects on ground signal intensity for sample transmitters. Our calculations indicate that ground-level field-intensity changes of several dB might be produced by joule-heating of the ionosphere by intense oblique HF waves. Our results are extremely sensitive to the model ionosphere and therefore indicate that an experiment should employ the widest possible range of frequencies and propagation conditions. — 2/2			
20. DISTRIBUTION/AVAILABILITY OF ABSTRACT <input type="checkbox"/> UNCLASSIFIED/UNLIMITED <input checked="" type="checkbox"/> SAME AS RPT <input type="checkbox"/> DTIC USERS		21. ABSTRACT SECURITY CLASSIFICATION Unclassified	
22a. NAME OF RESPONSIBLE INDIVIDUAL Paul Kossey		22b. TELEPHONE (Include Area Code)   22c. OFFICE SYMBOL   AFGL/LID	

SUMMARY

This volume presents numerical calculations of ionospheric electron density perturbations and ground-level signal changes for several electric field distributions produced by high-frequency (HF) transmitters. Plasma density perturbations are likely to occur in regions of intense electric field focusing. These shifts in the density and distribution of the plasma near the reflectrix may be manifested in measurable ground-level signal changes. We have simulated these interactions in our calculations.

Our analysis takes into account radio field focusing at caustics, the consequent joule-heating of the surrounding plasma, heat conduction, diffusion, and recombination processes--these being the effects of a powerful oblique "modifying" wave. We then seek effects on a secondary "test" wave which is propagated along the same path as the first. The test wave could, in fact, be the modifying wave itself, in which case the calculation would be of the "self-effect" of a powerful transmitter.

Our calculations indicate that ground-level field-intensity changes of several dB might be produced by joule-heating of the ionosphere by intense oblique HF waves. Although small, these calculated changes are similar to the 3 dB change measured by Bochkarev and associates [1,2,3,4], who gave only sketchy details of their experimental parameters. Our results are extremely sensitive to the model ionosphere and therefore indicate that an experiment should employ the widest possible range of frequencies and propagation conditions. An effective power of 90 dBW is far more likely to produce a detectable signal change than 85 dBW.



<b>Accession For</b>	
NTIS GRA&I	<input checked="" type="checkbox"/>
DTIC TAB	<input type="checkbox"/>
Unannounced	<input type="checkbox"/>
Justification	
By _____	
Distribution/	
<b>Availability Codes</b>	
Dist	Avail and/or Special
A-1	

## PREFACE

This volume applies theory developed in earlier work\* [5] to the problem of possible self-effects of powerful obliquely incident radio waves. Using the results from this earlier work, we use field-driven changes in ionospheric electron density to calculate modified ambient refractive index profiles and the consequent effects on ground signal intensity for sample transmitters. This volume is not self-contained and should be used in conjunction with Vol. 1, which presents the underlying equations and defines the majority of the symbols.

---

\*Field, E. C., R. M. Bloom, and K. E. Heikes. *Ionospheric Heating with Oblique Waves*. Vol. 1. *Electron Density Perturbations*. Pacific-Sierra Research Corporation, Report 1864, September 1988. AFGL-TR-88-0336. **ADA216260**

CONTENTS

SUMMARY ..... iii

PREFACE ..... iv

FIGURES ..... vi

Section

  I. INTRODUCTION ..... 1

  II. TECHNIQUE OF CALCULATION ..... 2

  III. EXAMPLES ..... 6

  IV. CONCLUSIONS ..... 36

REFERENCES ..... 37

## FIGURES

1a. Model antenna patterns .....	7
1b. Model ionospheric profiles .....	8
2a. Ray trace, curtain antenna, 17.75 MHz, day .....	9
2b. Ray trace, curtain antenna, 9.7 MHz, night .....	10
2c. Ray trace, Bochkarev model, 15 MHz, day .....	11
3a. $E^2/Ep^2$ for curtain antenna, 17.75 MHz, day .....	12
3b. $E^2/Ep^2$ for curtain antenna, 9.7 MHz, night .....	13
3c. $E^2/Ep^2$ for Bochkarev model, 15 MHz, day .....	14
4a. Fractional change in electron temperature, curtain antenna, 17.75 MHz, day .....	18
4b. Fractional change in electron temperature, Bochkarev model, 15 MHz, day .....	19
5a. Fractional change in electron density, curtain antenna, 17.75 MHz, day .....	20
5b. Fractional change in electron density, curtain antenna, 9.7 MHz, night .....	21
5c. Fractional change in electron density, Bochkarev model, 15 MHz, day .....	22
6. Geometry of the diffusion calculation .....	24
7a. Change in ground field intensity, curtain antenna, 17.75 MHz, day .....	25
7b. Change in ground field intensity, curtain antenna, 9.7 MHz, night .....	26
7c. Change in ground field intensity, Bochkarev model, 15 MHz, day .....	27
8. Steps in intensity change calculation, curtain antenna ....	29
9a. Ground effect versus power-gain, Bochkarev model, 15 MHz, day, 60° dip .....	30

9b.	Ground effect versus power-gain, Bochkarev model, 15 MHz, day, 60° dip. (Trend illustrating prediction of linear theory in nonlinear regime, 95 dBW.) .....	31
10.	Ground effect versus dip angle, Bochkarev model, 15 MHz, day, 85 dBW .....	32
11.	Change in arrival angle versus power-gain, Bochkarev model, 15 MHz, day, 60° dip .....	34
12.	Change in arrival angle versus dip angle, Bochkarev model, 15 MHz, day, 85 dBW .....	35

## I. INTRODUCTION

Volume I of this report [5] derived equations for the electron density perturbations produced by an oblique angle ionospheric heater, and presented some results for idealized heating functions that allowed analytic solutions. This volume presents numerical calculations of ionospheric electron density perturbations and ground-level signal changes for several spatial electric field distributions produced by HF transmitters. We have assumed antenna patterns and power-gain products based on large shortwave broadcast transmitters, such as the new Voice of America facilities (e.g., [6]). We employ simplified daytime and nighttime two-layer ionospheric profiles.

It is the nature of oblique propagation that electric fields focus strongly into *caustics* which compensate for signal loss due to geometric spreading [7,8]. The significant region of intense focusing occurs along the Ray-Bundle, just beyond the wave-group reflection height in the ionosphere. What plasma density perturbations may occur as a result of the field are therefore likely to be most pronounced in the vicinity of this region. It is reasonable to assume that even subtle shifts in the density and dimension of the plasma near the reflectrix will be manifested in more profound effects in *ground-level* signal strength--in particular, at the edge of the geometrical shadow. It is this effect which our calculations are designed to measure.

Our analysis takes into account radio field focusing at caustics, the consequent joule-heating of the surrounding plasma, heat conduction, diffusion, and recombination processes--these being the effects of a powerful oblique "modifying" wave. We then seek effects on a secondary "test" wave, which is propagated along the same path as the first. The test wave could, in fact, be the modifying wave itself, in which case the calculation would be of the "self-effect" of a powerful transmitter.

In essence, our approach means recalculating an electric field distribution using an index of refraction modified by the intense

wave. Our calculations are grounded in what might be called a "first-order" approximation to nonlinear wave propagation. We have, moreover, omitted from the analysis dependence of kinetic and recombination coefficients on temperature. The controlling hypothesis is that, should first-order calculations fail to produce notable heating effects, nonlinear effects on collision frequency and diffusion would probably not increase the magnitude of the heating to a detectable level. Certain nonlinear phenomena, such as plasma instabilities, might produce detectable effects omitted from the linear theory.

## II. TECHNIQUE OF CALCULATION

Our calculations are accomplished through an aggregation of three separate procedures, each producing a set of data utilized as input by the next procedure. The first, which we shall call "Caustic" [9], computes an electric field distribution, given an oblique transmitter and a horizontally stratified ionospheric profile. The Caustic calculation evaluates the electric field as a superposition of quasi-plane-wave components, each component being an asymptotic solution to the wave equation in a medium with specified (field-independent) refractive index. The Caustic calculation, unlike standard first-order WKB asymptotics, is uniformly valid, that is, both in the region of geometrical optics and across caustics. This method allows us to calculate field magnitudes throughout large regions of space without having to piece together boundary conditions and different asymptotics inside and outside areas of strong focusing. When we calculate the wave field resulting from refraction through a perturbed, no longer horizontally stratified ionosphere, a less accurate method than Caustic must be used to estimate field intensity.

The second procedure is the "Diffusion" calculation, utilizing the steady-state solution Eq. (19)\* for electron density perturbation. The electric field intensity data  $E(x,z)$  from Caustic is converted to data  $E(x,z')$ , where  $z'$  designates a coordinate in the direction of the local magnetic field; we have been examining, primarily, east-west propagation, and thus  $z'$  lies in a plane perpendicular to the direction of propagation. It is assumed that the only significant plasma diffusion will occur in the  $z'$  direction. Average values for the coefficients  $L_N$ ,  $L_T$ , etc. in Eq. (19) are obtained from empirical models of the height dependence of ambient electron recombination coefficients and electron temperature [10]. Equation (19) is then evaluated for  $n/N_0$ , the relative change in electron density, by numerical integration. In an identical manner, the data  $E(x,z')$  can

---

\*All equation numbers lower than 46 refer to equations in Vol. 1.

be used to evaluate the relative change in electron temperature  $\Delta T/T_0$  by numerically integrating Eq. (8). It is Eq. (19) and  $n/N_0$ , though, that ultimately we are interested in applying.

The last procedure in the calculation is the estimation of the ground-level electric field intensity change (in the "test" wave) due to ionospheric perturbation  $n/N_0$ . As mentioned above, the "Caustic" calculation cannot accommodate ionospheric profiles that have gradients in other than the vertical ( $z$ ) direction. This is now the case: we are given to consider the propagation problem through a medium with "modified" complex polarizability  $\sigma'(x, z) = \sigma_0(z)(1 + n/N_0)$ . It is here that ray tracing and geometrical optics calculations serve best. A well-tested ray tracing program [11] is used, first with refractive index  $N(z)$ , then with  $N'(x, z)$ . In conjunction with the ray trace, we integrate certain quantities measuring the rate of change of ray coordinate with respect to infinitesimal changes in ray initial conditions (i.e., launch and azimuth). This allows for the continuous calculation of the relative convergence of a small (infinitesimal) pencil of rays around the main ray. This convergence (or divergence) factor is proportional to the electric field intensity at a point. Conservation of energy along ray tubes justifies this calculation. The product of the component of the Poynting vector in the direction of local group velocity and an infinitesimal ray tube area is constant over the ray path. As ray tube area shrinks with focusing, the field intensity grows proportionally. This calculation in fact, gives the slowly varying amplitude factor of the geometrical optics theory. We have followed the methods of Nickisch and Buckley [12,13].

We make this calculation on the ground for both the regular and perturbed ionosphere and obtain the change in field intensity. Several points must be stressed. First, the geometrical optics field intensity becomes unbounded at the skip distance, both at the interior caustic and at the horizon. Analysis shows that the region of validity is wherever the fractional change in adjacent ray spacing in one wavelength is much less than one. The method may exhibit a shift in the interior skip distance, but cannot predict accurate

fields there, which may change on the order of 5 to 10 db. Second, in the illuminated region past the interior skip, there are typically two rays landing at each point. This gives rise to rapidly varying interference phenomena in the field amplitude depending strictly on the phase difference between the high and low rays at each point. The amplitude of the complete field lies in the envelope formed by the sum and difference of the component ray amplitudes. It may be assumed that the resultant amplitude is, on the average, the *root-mean-square* of the two components.

It should be noted that a related, though different, approach to weakly nonlinear wave propagation can be found in work by Bochkarev [1,2,3,4]. Here, the nonlinearity in dielectric constant is assumed, a priori, to be proportional to the electric field intensity  $|E|^2$ . That is,  $N'^2 = N^2 + \alpha|E|^2$ , where  $N$  is the refractive index and  $\alpha$  is the coefficient of nonlinearity. Except for the region immediately surrounding the caustic, the field is found by classical geometrical optics with the ambient refractive index  $N$ . The classical field is used as a boundary condition on a small rectangular domain around the caustic; therein, a technique known as the *Method of Parabolic Equations* is used to approximate the field close to rays [10]. It would appear that our method of solution has the advantage of providing insight into the constitution of the nonlinearity that Bochkarev has bottled up into the ad hoc constant  $\alpha$ .

For a treatment analogous to ours, with a deeper analysis of HF wave energy deposition, as well as estimates of nonlinear absorption due to plasma instabilities, see Meltz, Holway, and Tomljanovich [14]. Their work applies only to vertically incident waves. For an adaptation of this class of calculations to an automatic, feedback-propelled computational scheme, see Bernhardt and Duncan [15].

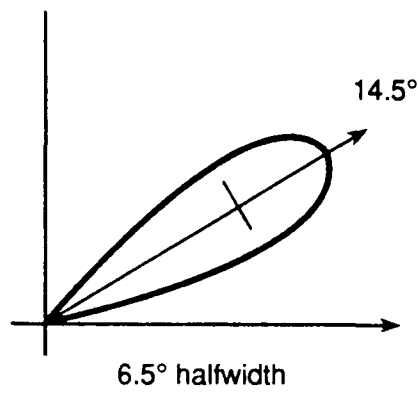
### III. EXAMPLES

We distinguish two calculations: the curtain antenna case, modeled to roughly approximate large HF facilities such as future VOA sites [6]; and the Bochkarev model, extracted from a series of articles [1,2,3,4] whose results we have used (with some skepticism) as a guide. Both day and nighttime ionospheres are treated for the curtain antenna model; whereas for the Bochkarev model we use only a daytime model ionosphere--as close to Bochkarev's as could be ascertained from the published account. In both cases, propagation is perpendicular to the magnetic field vector; the dip angle is  $60^\circ$ , corresponding to the middle latitudes.

The antenna patterns, transmitter power, and ionospheric profiles distinguishing these cases are shown in Figs. 1a and 1b. Sample ray traces, one for each profile, are shown in Figs. 2a through 2c. The fact that the curtain antenna profile is denser at its maximum (F2 layer at 300 km) than the Bochkarev profile (F2 layer at 250 km) means that the maximum usable frequency (MUF) for the given launch angle for the curtain antenna will be greater. Though the MUF for the Bochkarev model was not given in the published articles [3,4], by trial and error we found that 15 MHz was appropriate for the propagation path that was shown in the articles. We found that any degree of arbitrariness in the choice of ionospheric profile makes all but the grossest characteristics of subsequent calculations fluctuate substantially. In light of this strong sensitivity to model parameters, we are justified in abstracting from our calculations only a few general principles.

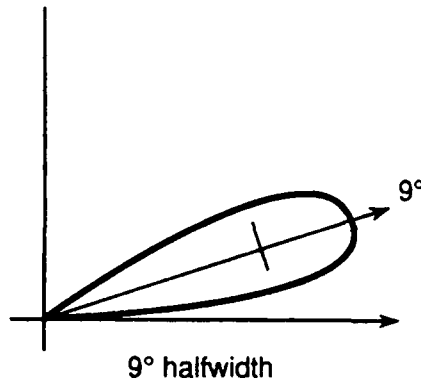
Figures 3a through 3c show the calculated electric field strength contours for the three cases. Each diagram is centered about the wave reflection height and caustic region; this can be seen by comparison with the corresponding ray traces. All of the indicated cases produce field strengths as large as several tenths of a volt per meter. The diffusion calculation then proceeds with the electric field data and various altitude-dependent parameters (see Table 2 in Vol. 1, Sec. 2).

a. Curtain antenna, day.



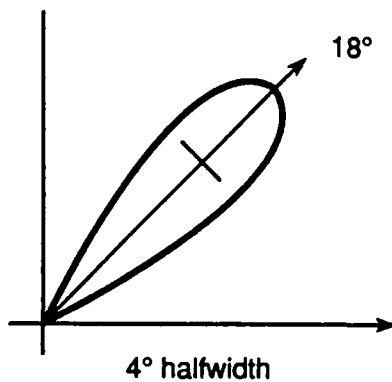
$f = 17.75 \text{ MHz}$   
21.5 dB maximum  
 $1.25 \times 10^6 \text{ watts}$   
80 dBW effective power

b. Curtain antenna, night.



$f = 9.75 \text{ MHz}$   
25 dB maximum  
 $10^6 \text{ watts}$   
85 dBW effective power

c. Bochkarev model.



$f = 15 \text{ MHz}$   
25 dB maximum  
 $10^6 \text{ watts}$   
85 dBW effective power

Figure 1a. Model antenna patterns.

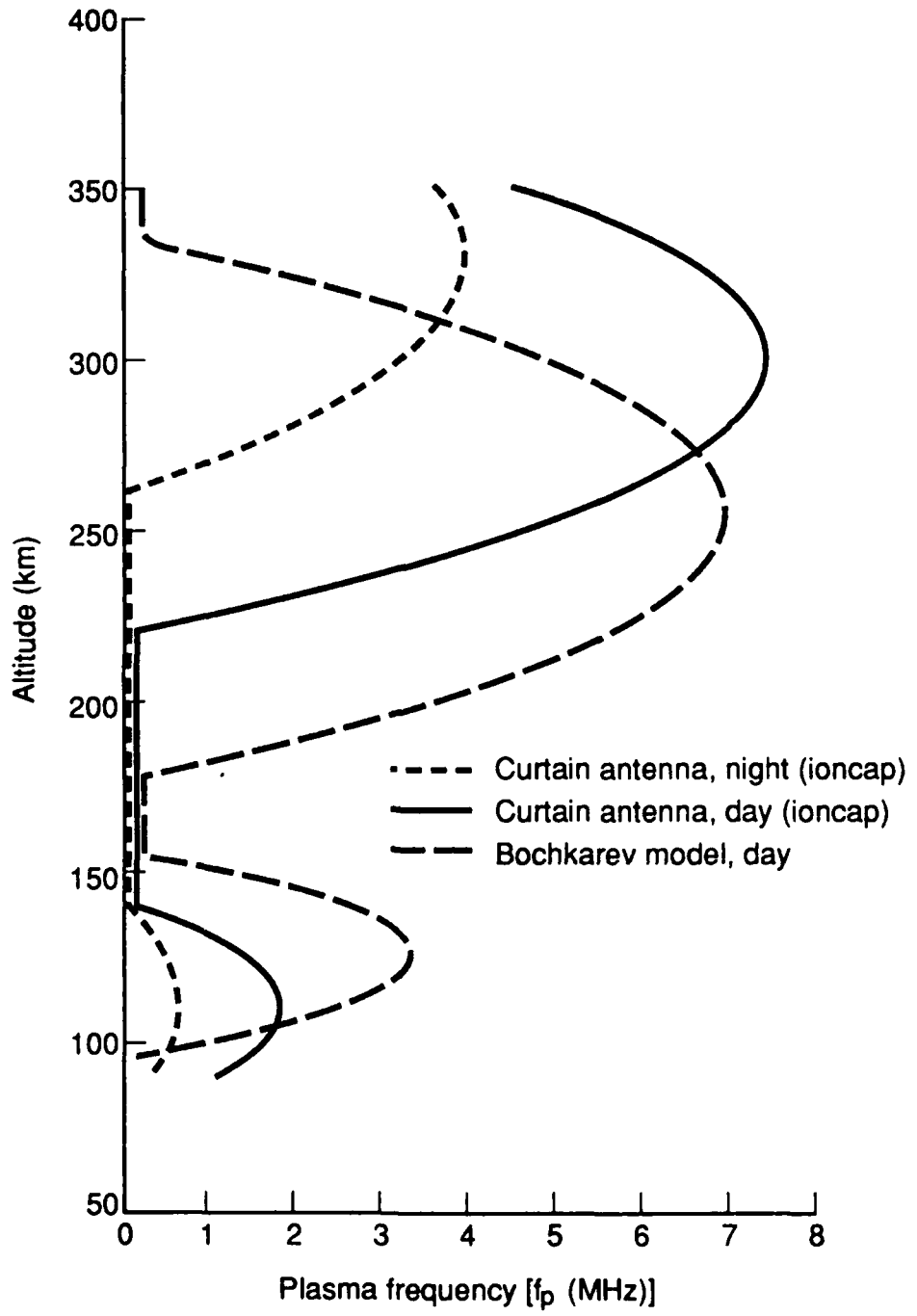


Figure 1b. Model ionospheric profiles.

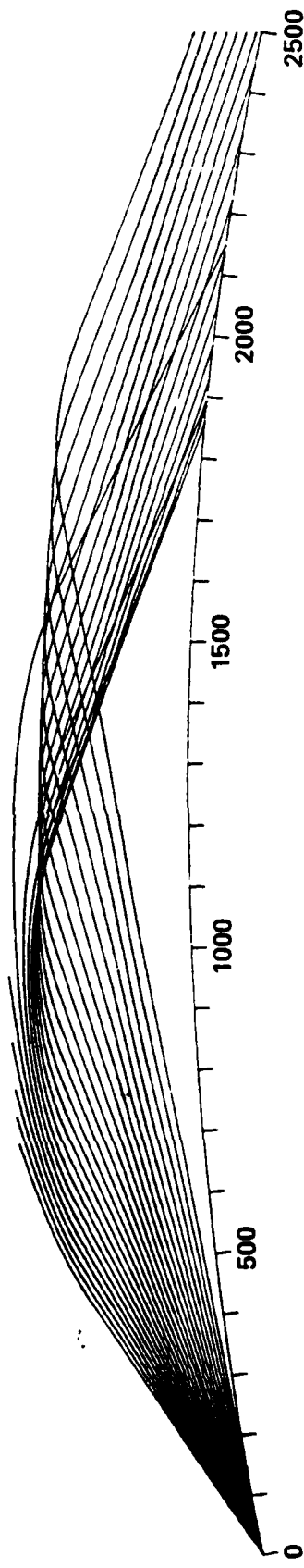


Figure 2a. Ray trace, curtain antenna, 17.75 MHz, day.

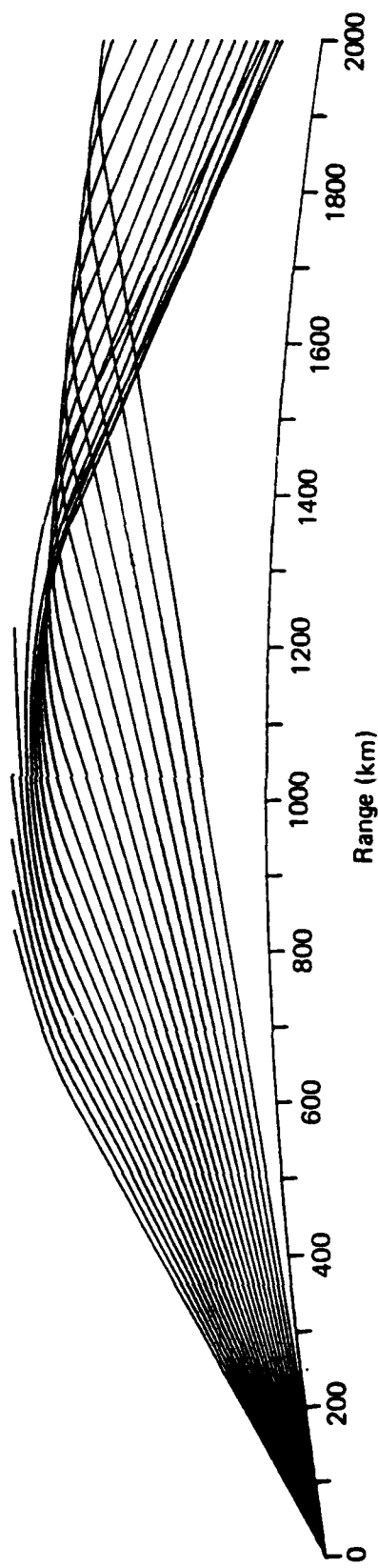


Figure 2b. Ray trace, curtain antenna, 9.7 MHz, night.

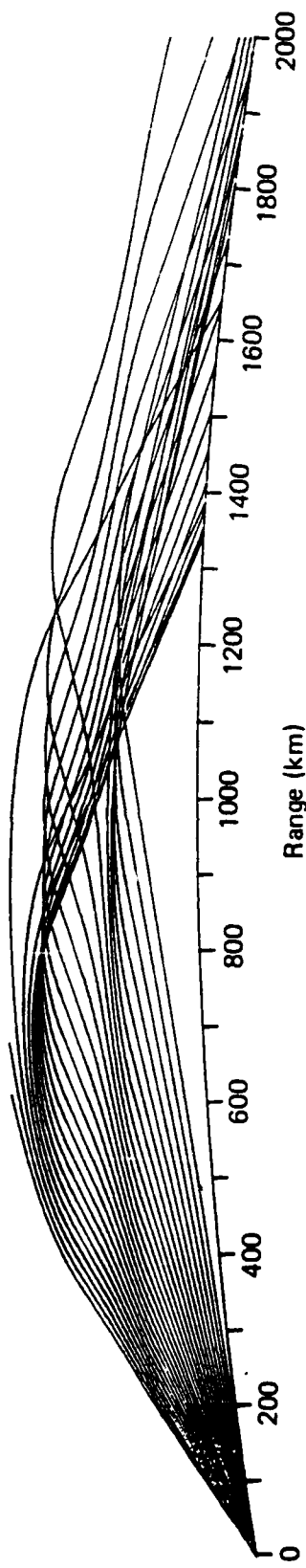


Figure 2c. Ray trace, Bochkarev model, 15 MHz, day.

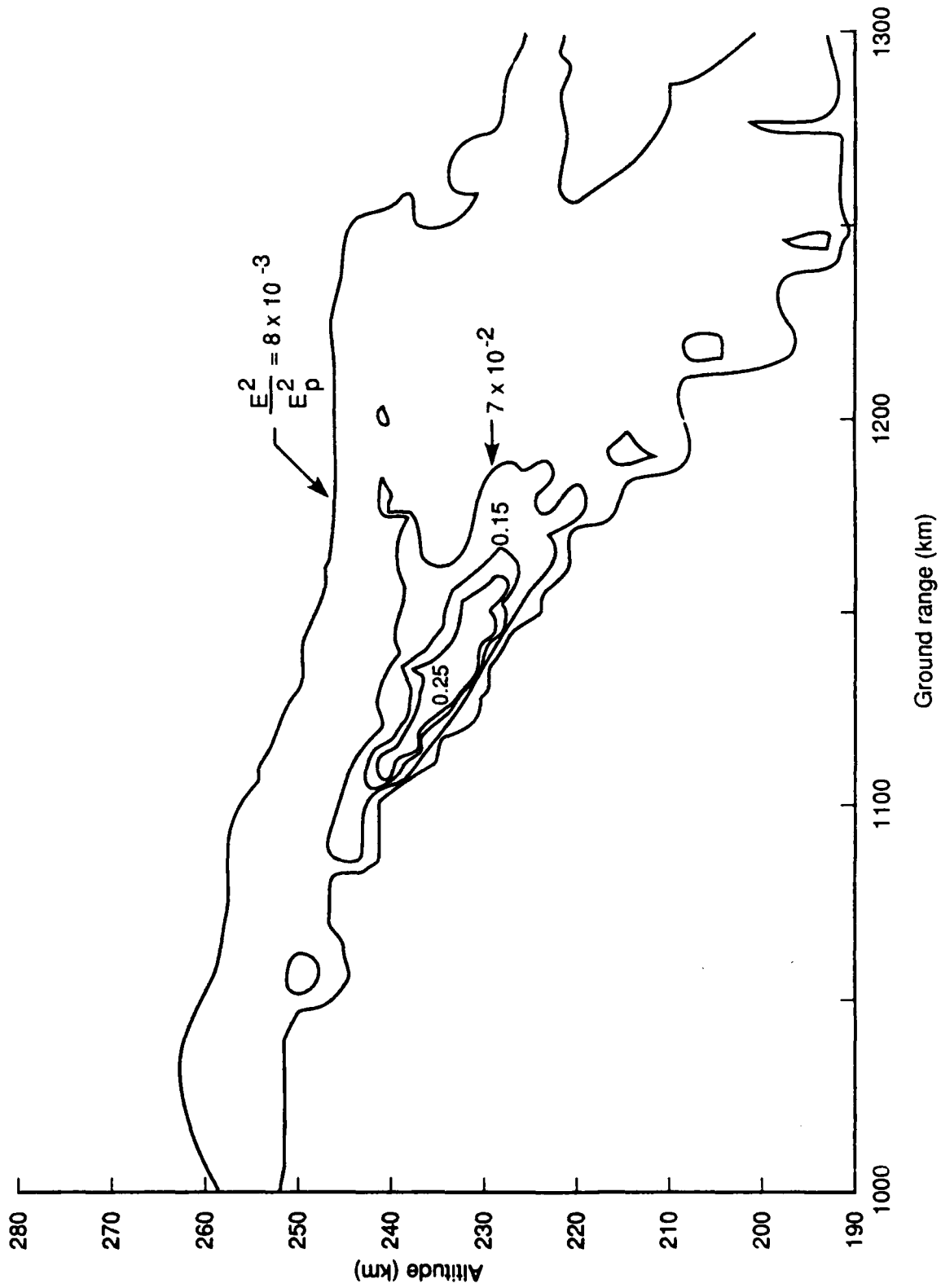


Figure 3a.  $E^2/E_p^2$  for curtain antenna, 17.75 MHz, day.

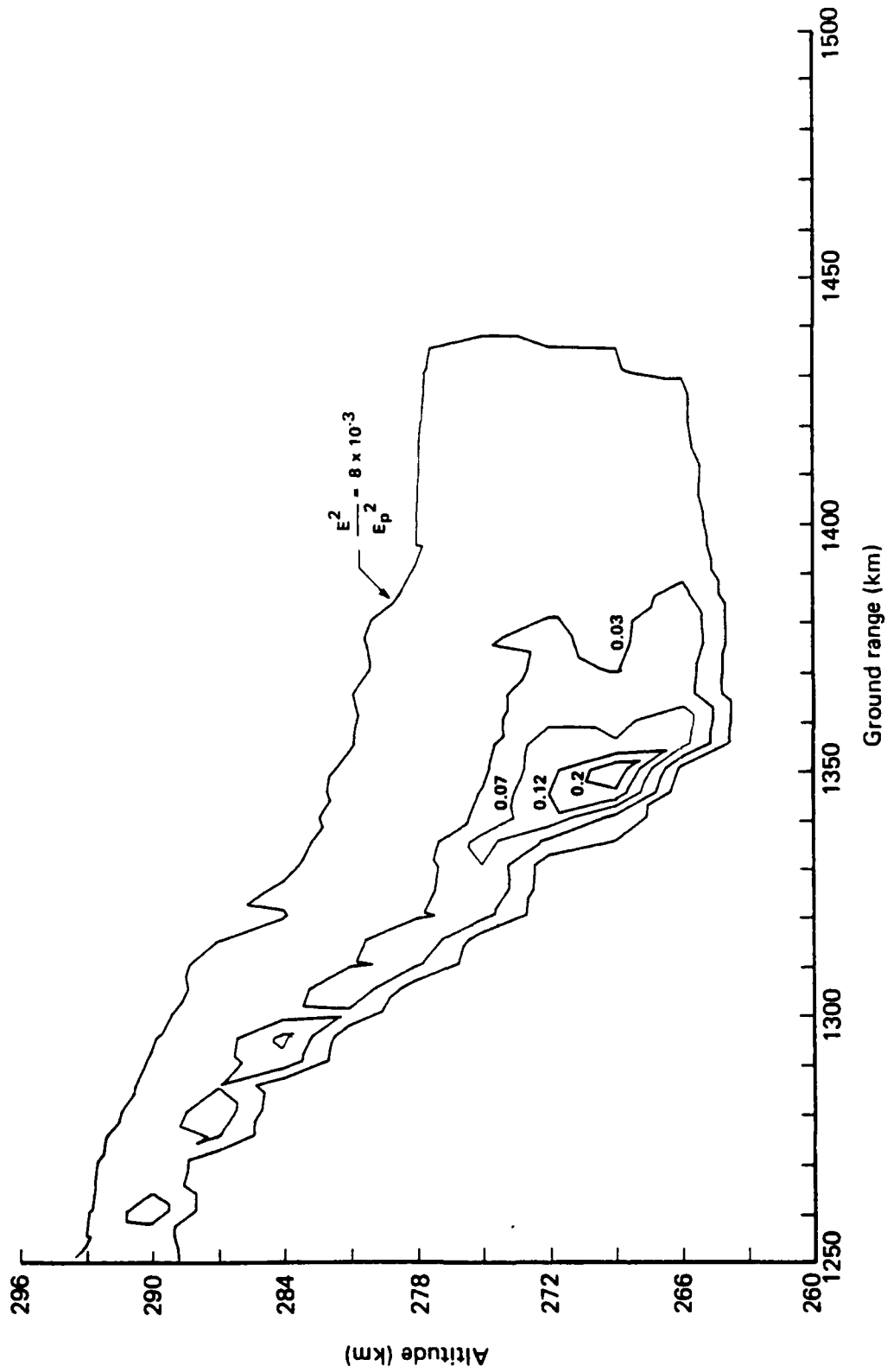


Figure 3b.  $E^2/E_p^2$  for curtain antenna, 9.7 MHz, night.

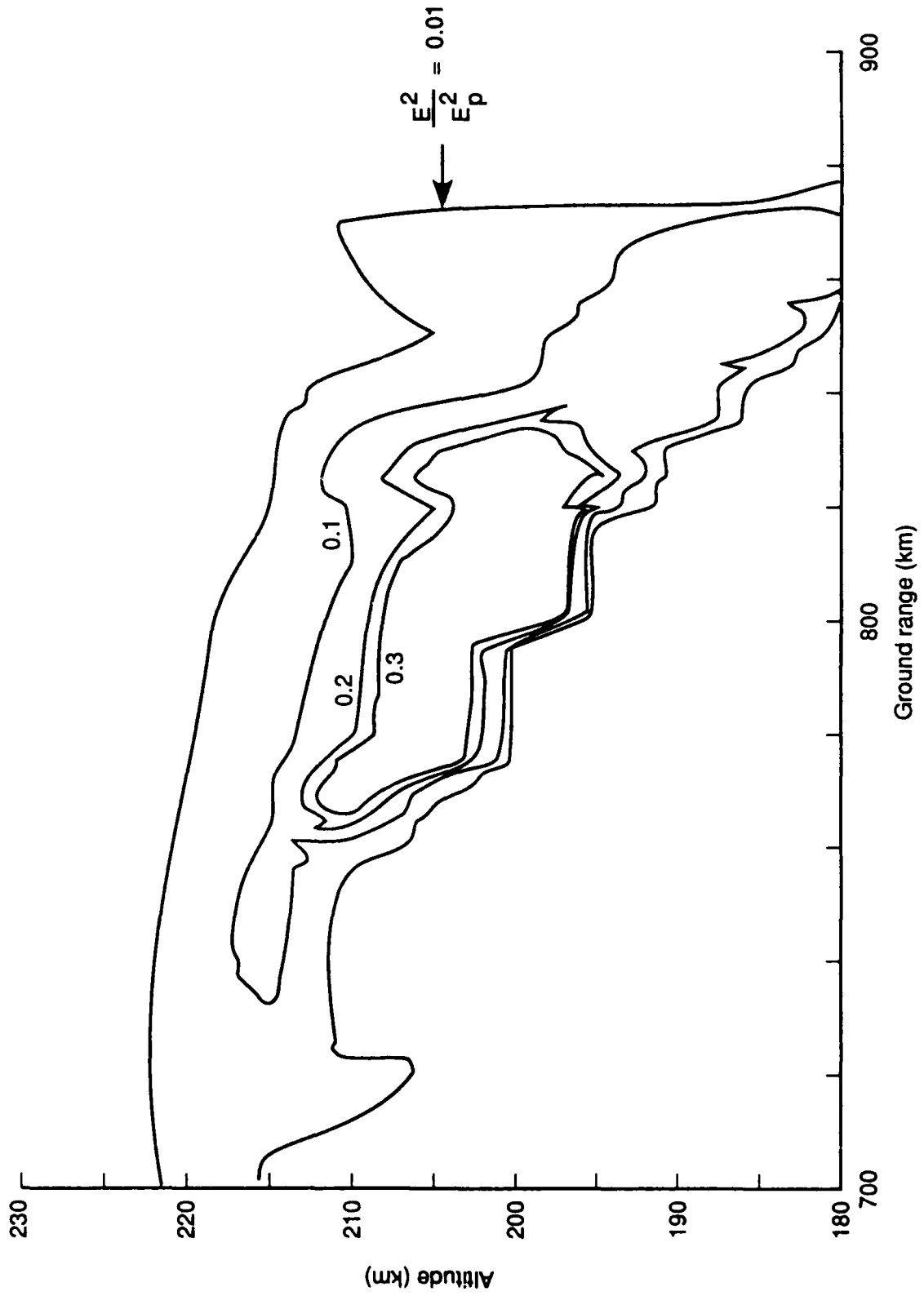


Figure 3c.  $E^2/E_p^2$  for Bochkarev model1, 15 MHz, day.

The quantity

$$E_p^2 = \frac{3T_e m \delta \omega^2}{e^2} . \quad (46)$$

is of primary interest, as the field  $E$  appears only in the combination  $E/E_p$  (Eq. [19]). We have used nominal values of electron temperature  $T_e$  versus altitude. To calculate  $\delta$ , the fractional loss of energy per electron per collision, we have used the formulations given in Table 1. The term  $(E/E_p)^2$  can be regarded as proportional to the energy in the propagating wave lost to kinetic heating of free electrons. At night  $E_p$  is somewhat larger than in the daytime, despite its proportionality to  $\omega$ ; that behavior occurs because the quantity  $\delta$  comes to be dominated by collisions with atomic oxygen at night (as opposed to elastic collisions with ions in the daytime).

Table 2 gives nominal parameter values. In order to perform the calculations we interpolated from the values in Table 1 to obtain values near the altitude of largest electric field. Figures 4a and 4b show electron temperature changes caused by the electric fields in Figs. 3a and 3b. The maximum temperature changes are on the order of a few percent for the curtain antenna daytime model, and a few tens of percent for the Bochkarev model. The difference in results for those two models indicates the extreme sensitivity to ionospheric parameters and transmitter characteristics.

Figures 5a through 5c show the calculated relative electron density perturbations,  $n/N_0$ , which are not larger than a few percent, and usually are smaller than that. Those values can be compared to the estimates obtained in Vol. 1, Sec. IV, Eqs. (38) through (44), for an idealized square heated region. Using Fig. 3c as an example, the most intensely heated spots extend over dimensions of several tens of kilometers, whereas  $(E/E_p)^2$  is on the order of 0.30. From Eq. (44) we have the estimate:

TABLE 1. Parameters For Diffusion Calculation.

$$\delta = \frac{\delta_{ei} \nu_{ei} + \delta_{e0} \nu_{e0}}{\nu_{e0} + \nu_{ei}}$$

$$\delta_{ei} = \frac{2M_e}{M_i} = 6.8 \times 10^{-5} \quad (\text{elastic collisions assumed})$$

$$\nu_{ei} = 6.1 \times 10^{-3} N_i (T_e / 300^\circ)^{-3/2} \quad [16]$$

$$\delta_{e0} = 82/T_0 \sqrt{T_e} \quad [10]$$

$$\nu_{e0} = 2.8 \times 10^{-10} N_0 \sqrt{T_e} \quad [10]$$

$$E_p^2 = \frac{3T_e m_e \delta}{e^2} \omega^2 \quad \left\{ \begin{array}{l} m_e = 9.1 \times 10^{-31} \text{ kg} \\ e = 1.602 \times 10^{-19} \text{ C} \\ \omega = 2\pi \times 10^6 \text{ f (MHz)} \end{array} \right.$$

TABLE 2. Ionospheric Parameters.

<u>DAY</u>							
<u>z (km)</u>	<u>T<sub>O</sub></u>	<u>T<sub>e</sub></u>	<u>N<sub>O</sub></u>	<u>N<sub>e</sub></u>	<u>ν<sub>ei</sub></u>	<u>ν<sub>e0</sub></u>	<u>δ<sub>e0</sub></u>
150	670	800	1.3×10 <sup>10</sup>	3×10 <sup>5</sup>	4.8×10 <sup>2</sup>	1.1×10 <sup>2</sup>	4.3×10 <sup>-3</sup>
200	1070	1100	3×10 <sup>9</sup>	5×10 <sup>5</sup>	4.4×10 <sup>2</sup>	31	2.3×10 <sup>-3</sup>
250	1250	1300	1.3×10 <sup>8</sup>	1.6×10 <sup>6</sup>	4.4×10 <sup>2</sup>	15	2×10 <sup>-4</sup>
300	1330	1400	5.9×10 <sup>8</sup>	1.5×10 <sup>6</sup>	6.5×10 <sup>2</sup>	7.3	1.6×10 <sup>-3</sup>
<u>NIGHT</u>							
<u>z (km)</u>	<u>T<sub>O</sub></u>	<u>T<sub>e</sub></u>	<u>N<sub>O</sub></u>	<u>N<sub>e</sub></u>	<u>ν<sub>ei</sub></u>	<u>ν<sub>e0</sub></u>	<u>δ<sub>e0</sub></u>
150	650	670	1.4×10 <sup>10</sup>	2.4×10 <sup>3</sup>	6.5	100	4.8×10 <sup>-3</sup>
200	850	900	3.2×10 <sup>9</sup>	3×10 <sup>3</sup>	5.8	27	3.2×10 <sup>-3</sup>
250	910	1000	1.2×10 <sup>9</sup>	10 <sup>4</sup>	16	10	2.8×10 <sup>-3</sup>
300	930	1200	4.4×10 <sup>8</sup>	10 <sup>5</sup>	115	4.3	2.5×10 <sup>-3</sup>
<u>DAY</u>				<u>NIGHT</u>			
<u>z (km)</u>	<u>δ</u>	<u>E<sub>p</sub><sup>2</sup></u>	<u>δ</u>	<u>E<sub>p</sub><sup>2</sup></u>			
150	8.6×10 <sup>-4</sup>	.040f <sup>2</sup>	.0045	.175f <sup>2</sup>			
200	2.1×10 <sup>-4</sup>	.013f <sup>2</sup>	.0026	.135f <sup>2</sup>	(f in MHz)		
250	7.2×10 <sup>-5</sup>	.005f <sup>2</sup>	.0011	.064f <sup>2</sup>			
300	8.5×10 <sup>-5</sup>	.006f <sup>2</sup>	.0002	.014f <sup>2</sup>			

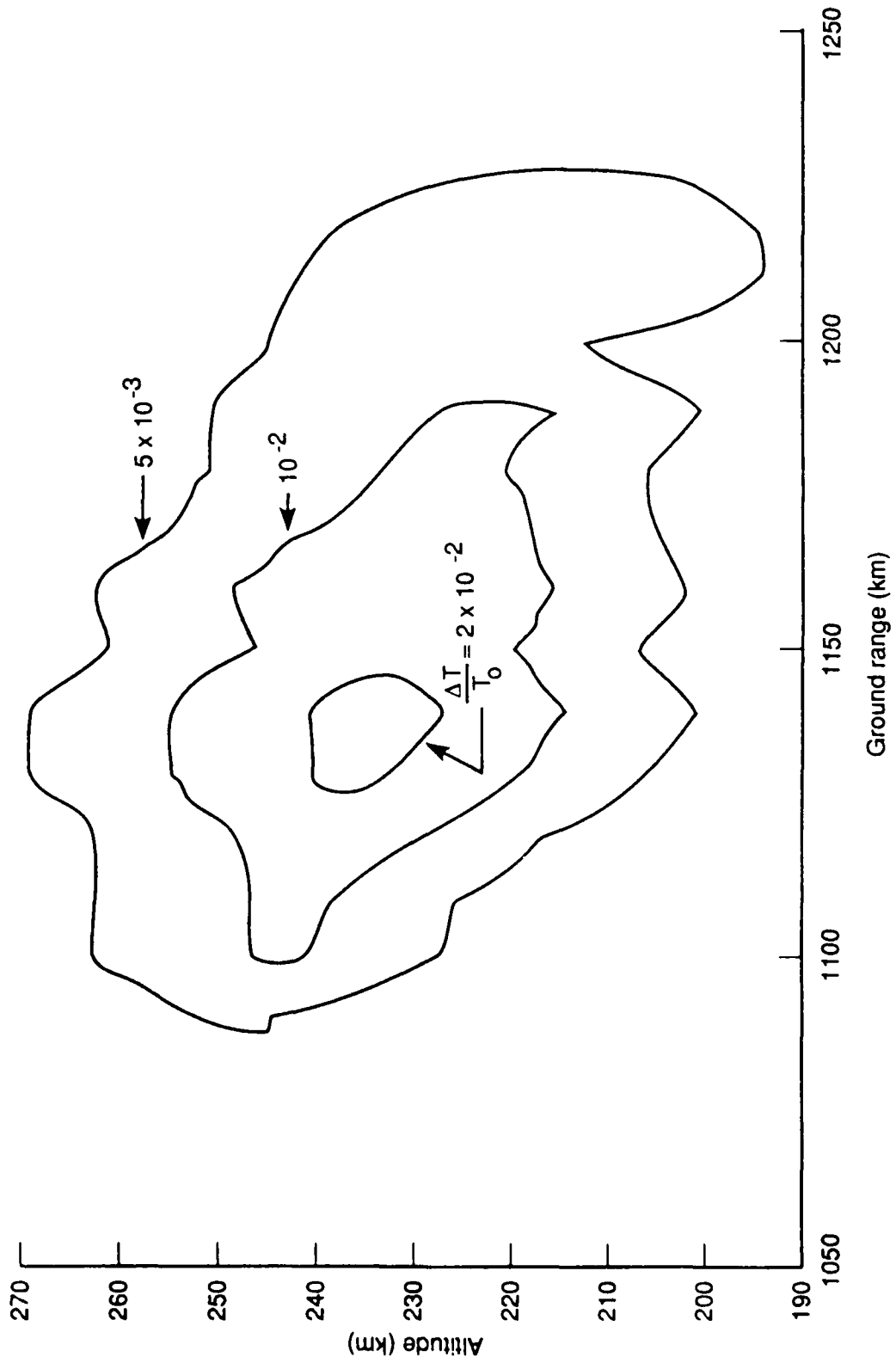


Figure 4a. Fractional change in electron temperature, curtain antenna, 17.75 MHz, day.

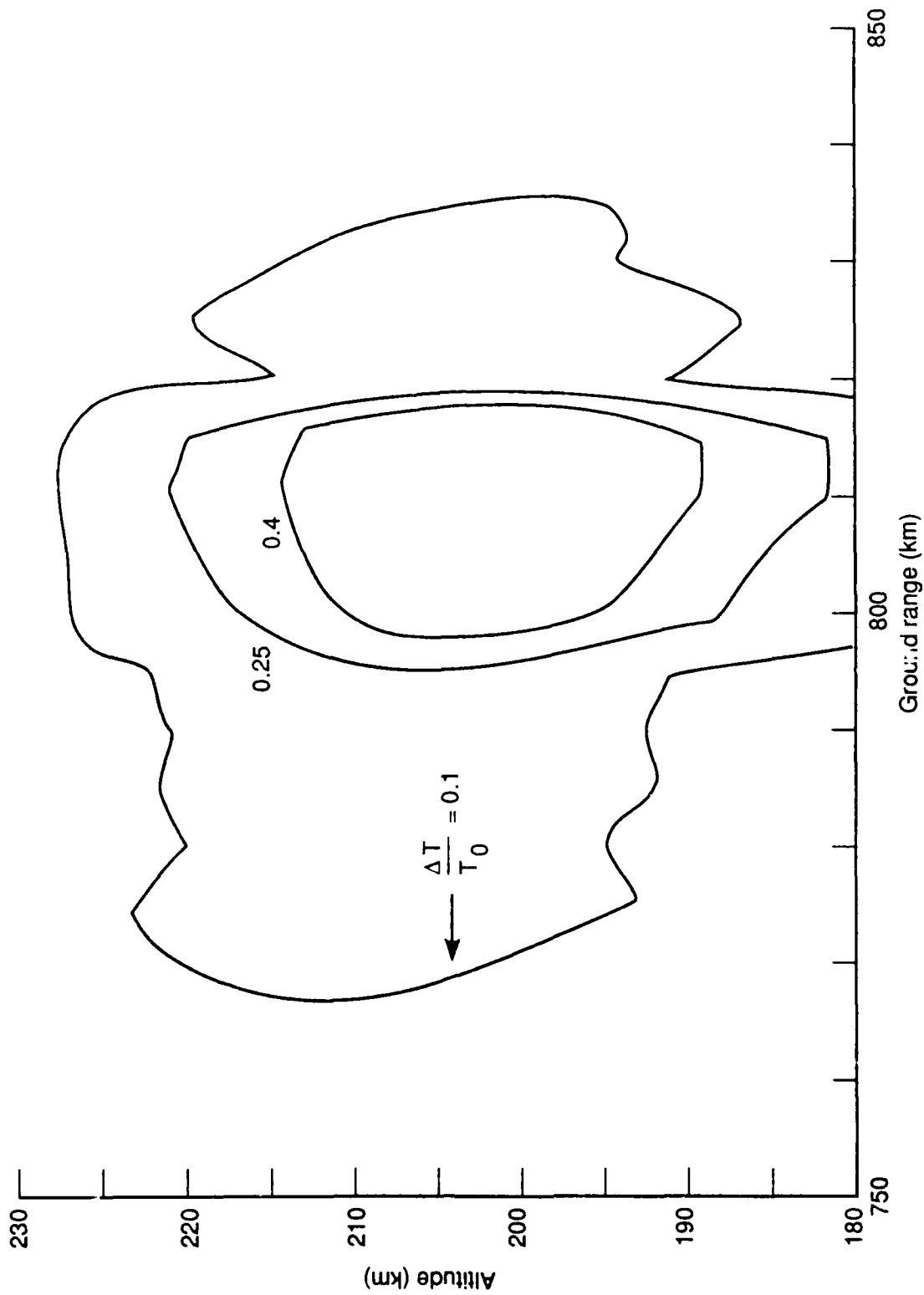


Figure 4b. Fractional change in electron temperature, Bochkarev model, 15 MHz, day.

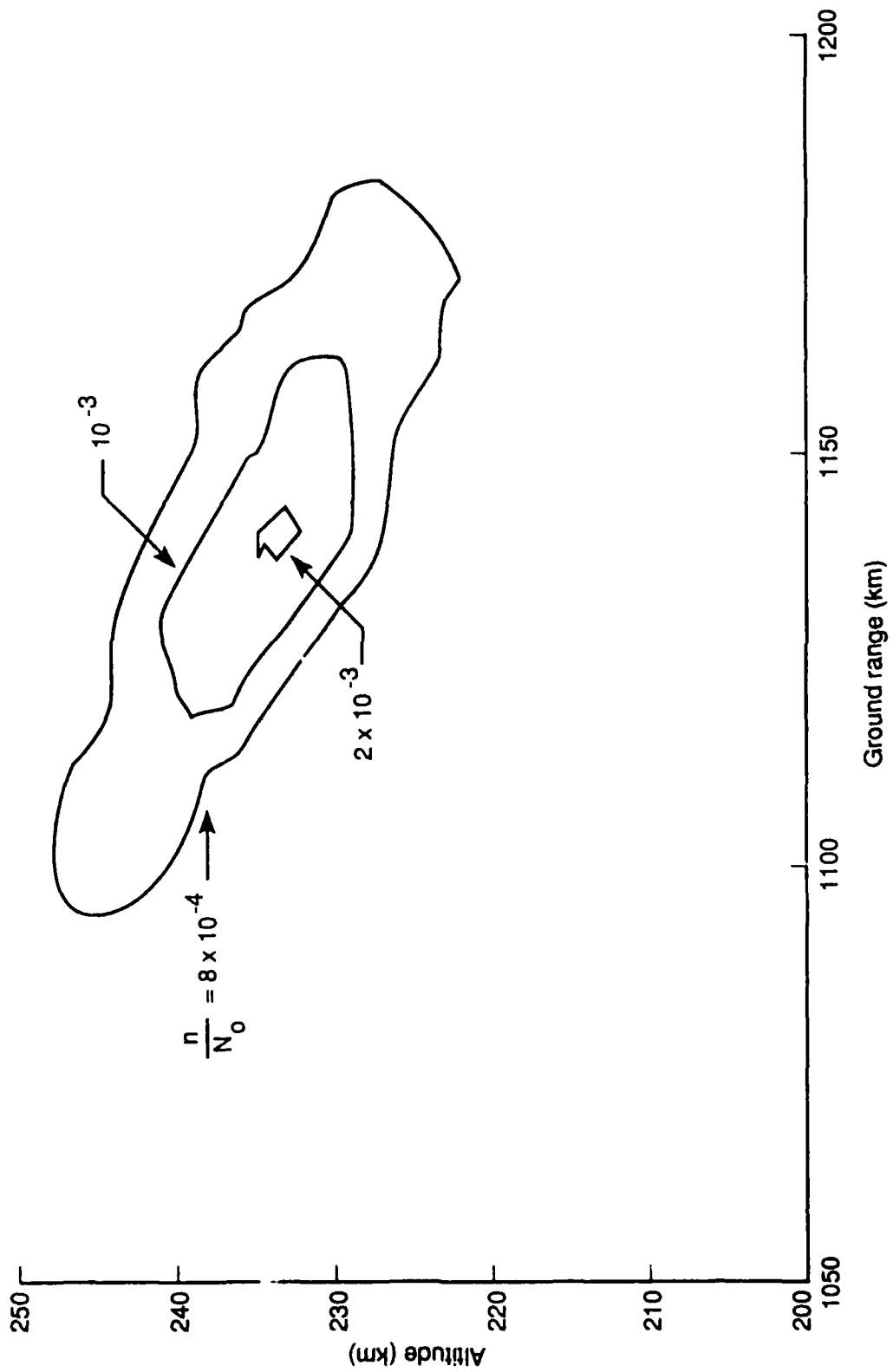


Figure 5a. Fractional change in electron density, curtain antenna, 17.75 MHz, day.

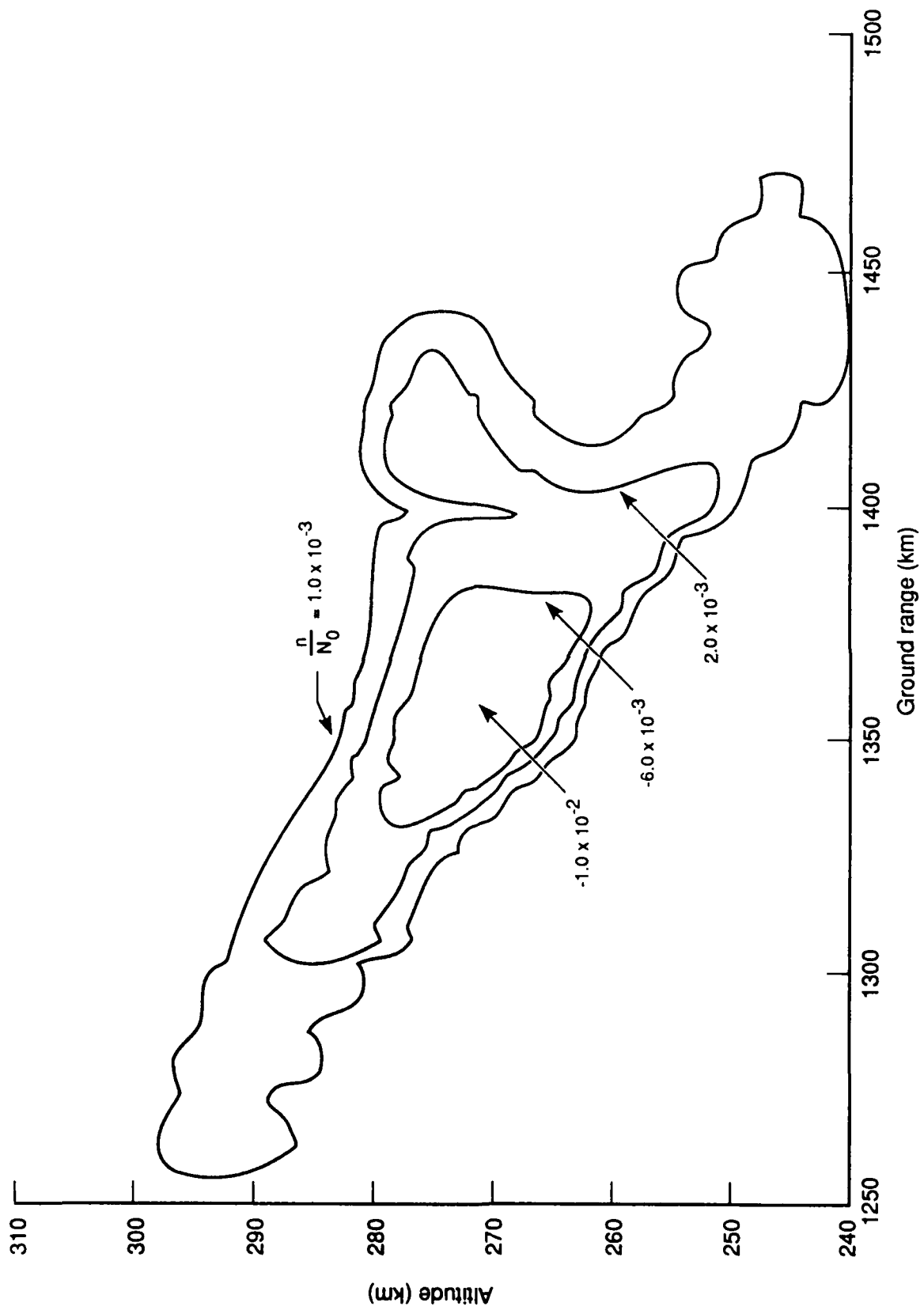


Figure 5b. Fractional change in electron density, curtain antenna, 9.7 MHz, night.

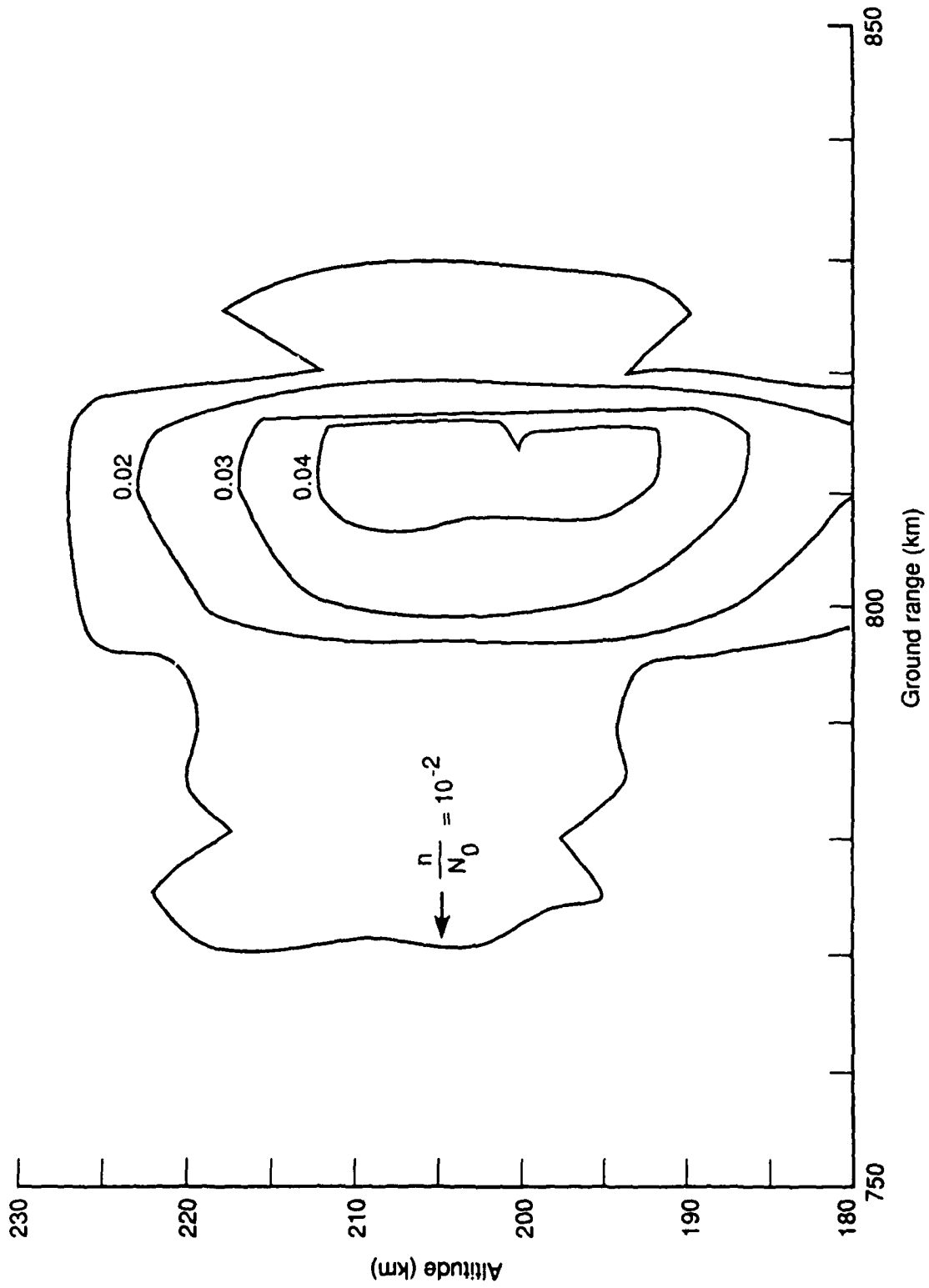


Figure 5c. Fractional change in electron density, Bochkarev model, 15 MHz, day.

$$\frac{n}{N_0} - R_T \frac{a}{L_T} \frac{L_N}{L_N + L_T} \frac{E^2}{E_P^2} \quad (48)$$

where  $a$  is the width of the heated region; and  $L_N$ ,  $L_T$ , and  $R_T$  are taken from Table 2, Vol. 1. Thus, taking  $a = 10$  km, and, for example, values of  $L_N$ ,  $L_T$ , and  $R_T$  for 250 km (9.2 km, 25 km, and .54), we see that this a priori estimate is 2 percent, which is close to our numerically calculated range of  $n/N_0$  shown in Fig. 5c. While the isocontours of field strength conform to the downward-curving pattern of the caustic, those of the density perturbation are elongated in roughly a vertical direction. This is because of our assumption that diffusion occurs only in the direction of the magnetic field lines (see Fig. 6).

Figure 7 shows the final result of the calculation. This is the change in the geometrical optics field intensity at the ground caused by the heater-induced ionospheric perturbation. Phase as a function of ground range is obtained by integrating the refractive index over the ray path. Power density as a function of ground range is calculated by Nickisch's method [12]. There are generally two or more rays, each with its own phase and amplitude, intersecting at a given ground point. Each amplitude-phase pair is regarded as a complex number. The resultant geometrical-optics field amplitude at such a ground point is given by the vector sum of these quantities. Once this resultant is calculated, for both perturbed and unperturbed profiles, it is a simple matter to interpolate the difference between both. The heater-induced intensity change, in dB (relative to  $1 \text{ V}^2/\text{m}^2$ ), is plotted in Figures 7a through 7c.

Notice that the predicted effects occur both in a region just past the skip distance, as well as several hundred kilometers beyond. Except at the skip distance, the predicted field-strength changes are small, ranging from about a dB change for the nighttime case (Fig. 7c) to about 2 dB for the daytime models (Figs. 7a and 7c). Where ray tube cross sections shrink to zero (that is, at the skip distance), this ray amplitude calculation is not reliable. Nickisch asserts that

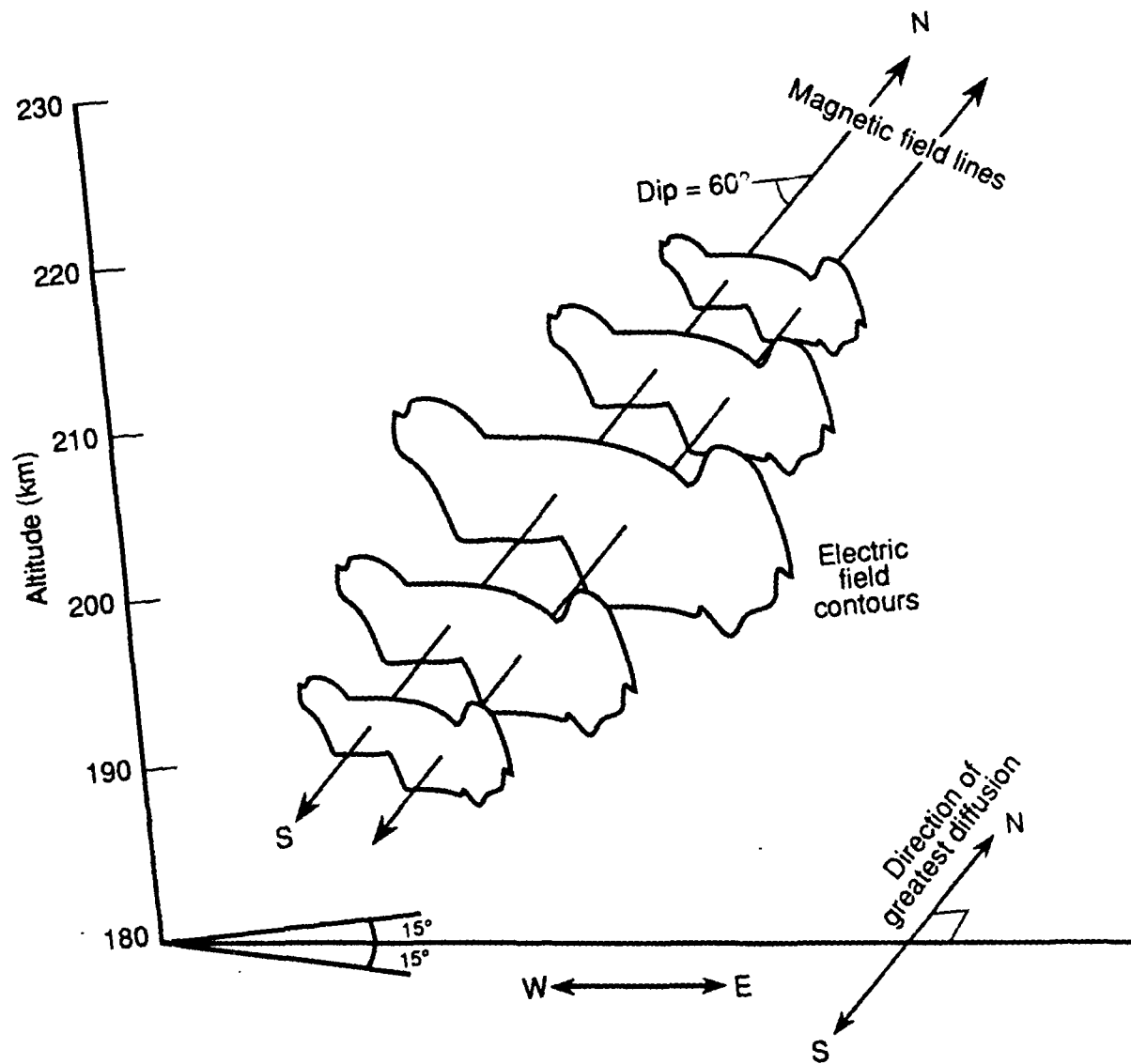


Figure 6. Geometry of the diffusion calculation.

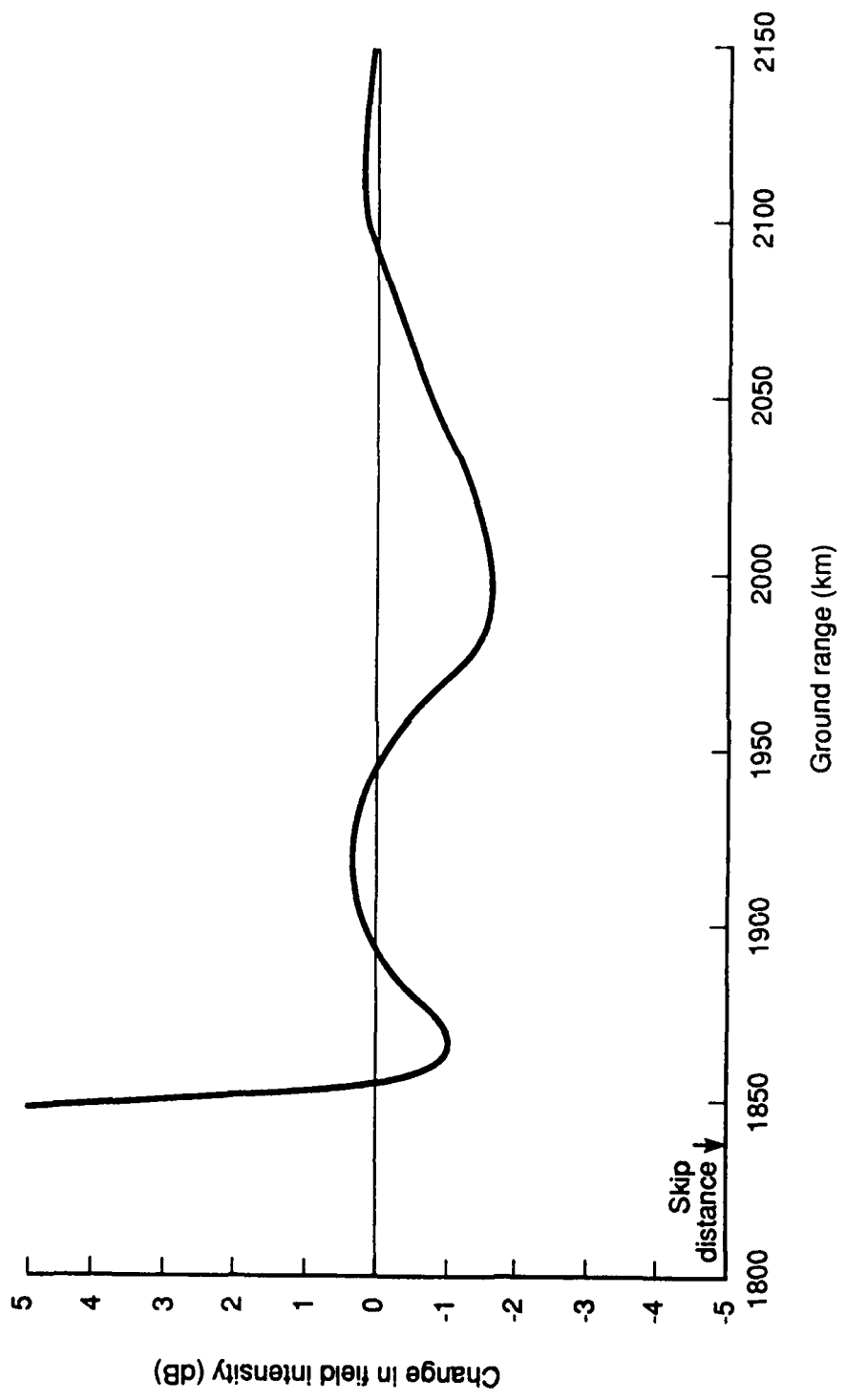


Figure 7a. Change in ground field intensity, curtain antenna,  
17.75 MHz, day.

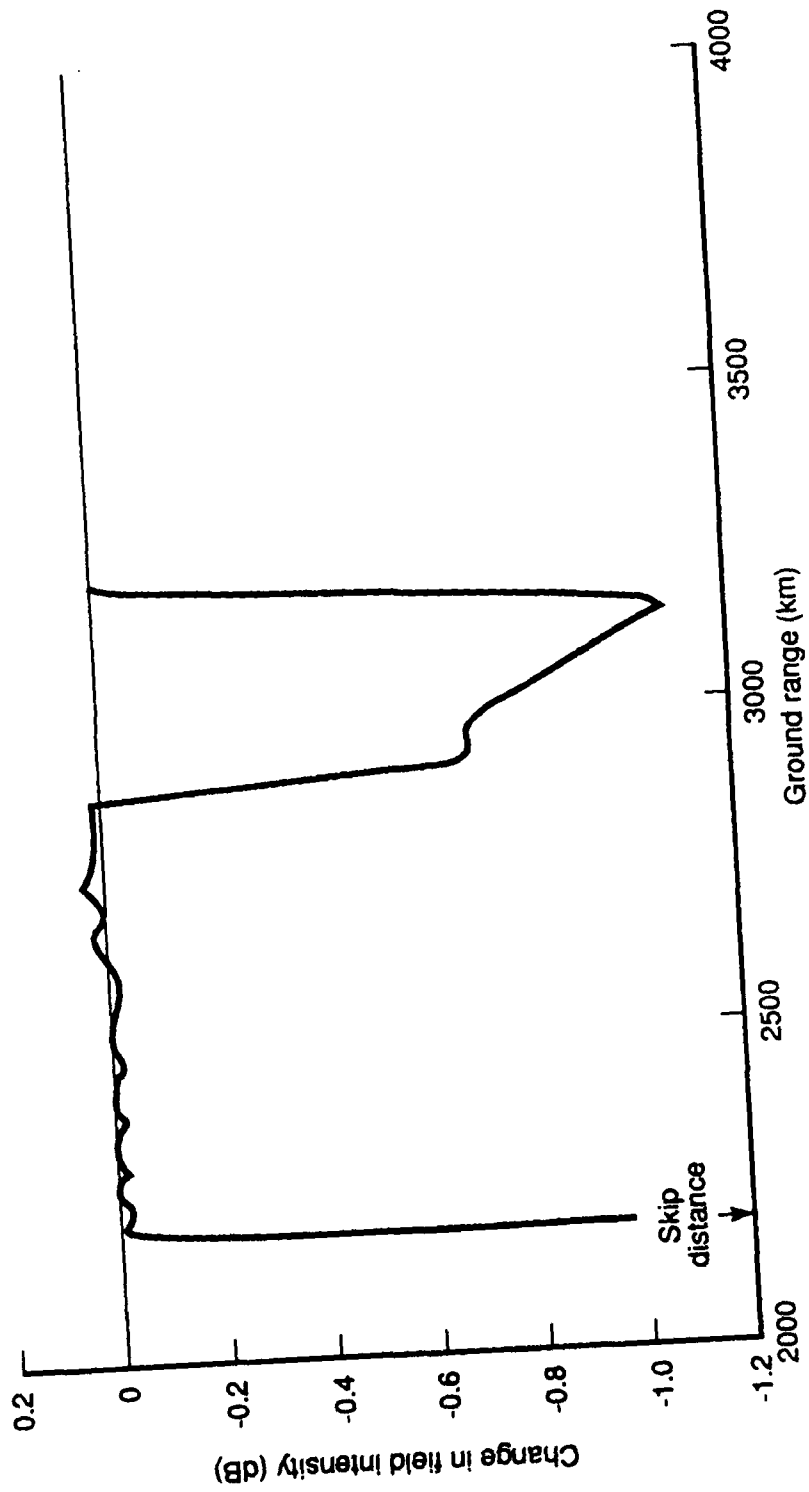


Figure 7b. Change in ground field intensity, curtain antenna, 9.7 MHz, night.

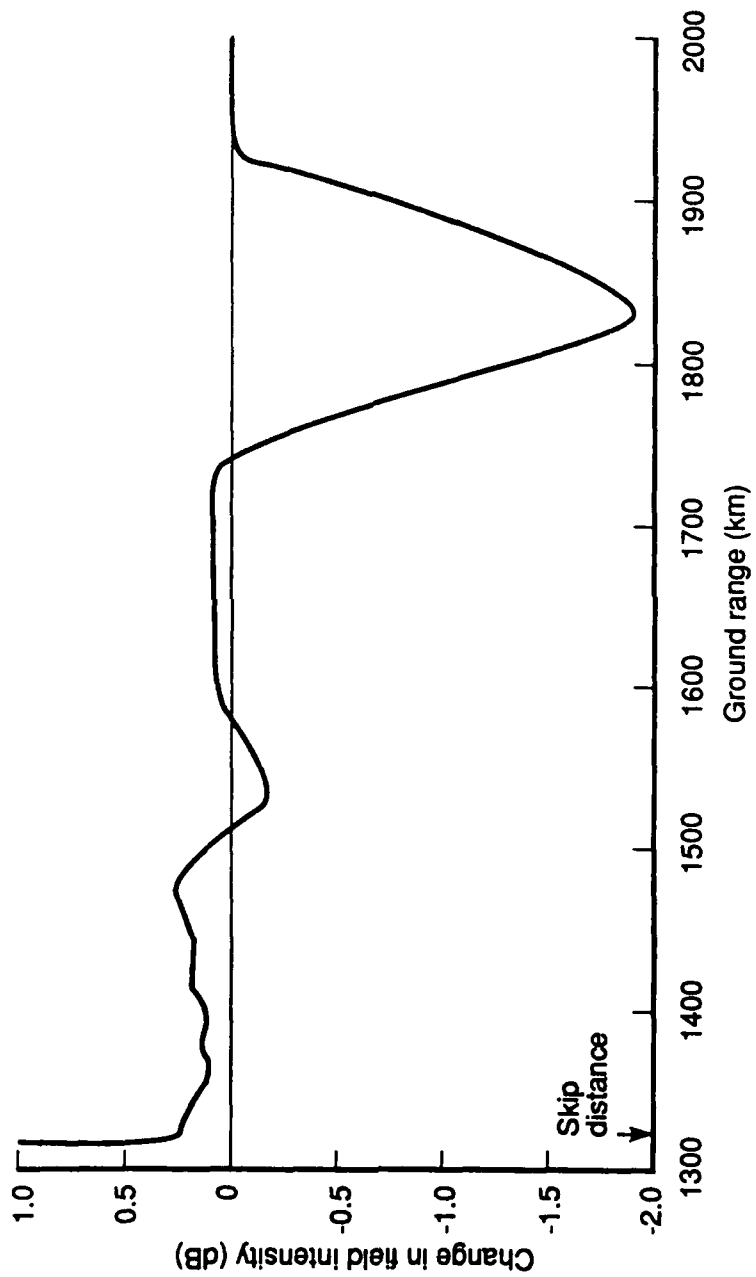


Figure 7c. Change in ground field intensity, Bochkarev model,  
1.5 MHz, day.

the power densities calculated by his method may be low by as much as 5 dB in the skip region. In any case, the calculated phases of interference phenomena at the skip will not be accurate enough to support detailed comparison of the modified and unmodified. (This is because the path-integrated refractive index is never a numerically accurate measure of plane-wave phase in the vicinity of a caustic [9]). The second region of noticeable intensity change is, however, far from both the interior caustic and from the horizon focus. Figure 7a shows a 2 dB fade centered 150 km past the skip; Fig. 7b shows about 2 dB 750 km past the skip; and Fig. 7c shows about 1 dB 500 km past the skip distance.

Figure 8 illustrates the steps comprising the intensity-change calculation for the daytime curtain antenna model. Notice the two amplitude components, corresponding to a high and a low ray. Far from the skip distance, there is only one such component.

The remaining figures (9 through 12) pertain to the 15 MHz daytime (Bochkarev) model and show various dependences of the ground-level signal.

Figure 9a indicates the trend in field-strength change as transmitter effective power is increased. As expected, the greater the effective power, the greater the field change. Although increasing power (a fortiori, increasing  $E^2/Ep^2$ ) much past the 85 dBW level results in an abuse of method (the differential equations we solve for  $n/N_0$  are only valid when  $E^2/Ep^2$  is much less than 1), one can infer that the 90 dBW prediction (where  $E^2/Ep^2 \sim 1$ ) gives an *upper bound* on effects which can occur as a result of *linear* kinetic processes alone. Figure 9b indicates the trend in this calculation once we are well beyond the region of applicability of the linear theory; here  $E^2/Ep^2$  is on the order of 10, and the predicted ground effect has increased by an order of magnitude.

Figure 10 shows the dependence of the ground-level field-strength change upon the local magnetic field dip angle. The direction of propagation has, herein, been taken as east-west. The diffusion decreases as the dip angle tends toward the horizontal, because the gradients in the field quantities in Eqs. (4) and (18) become essen-

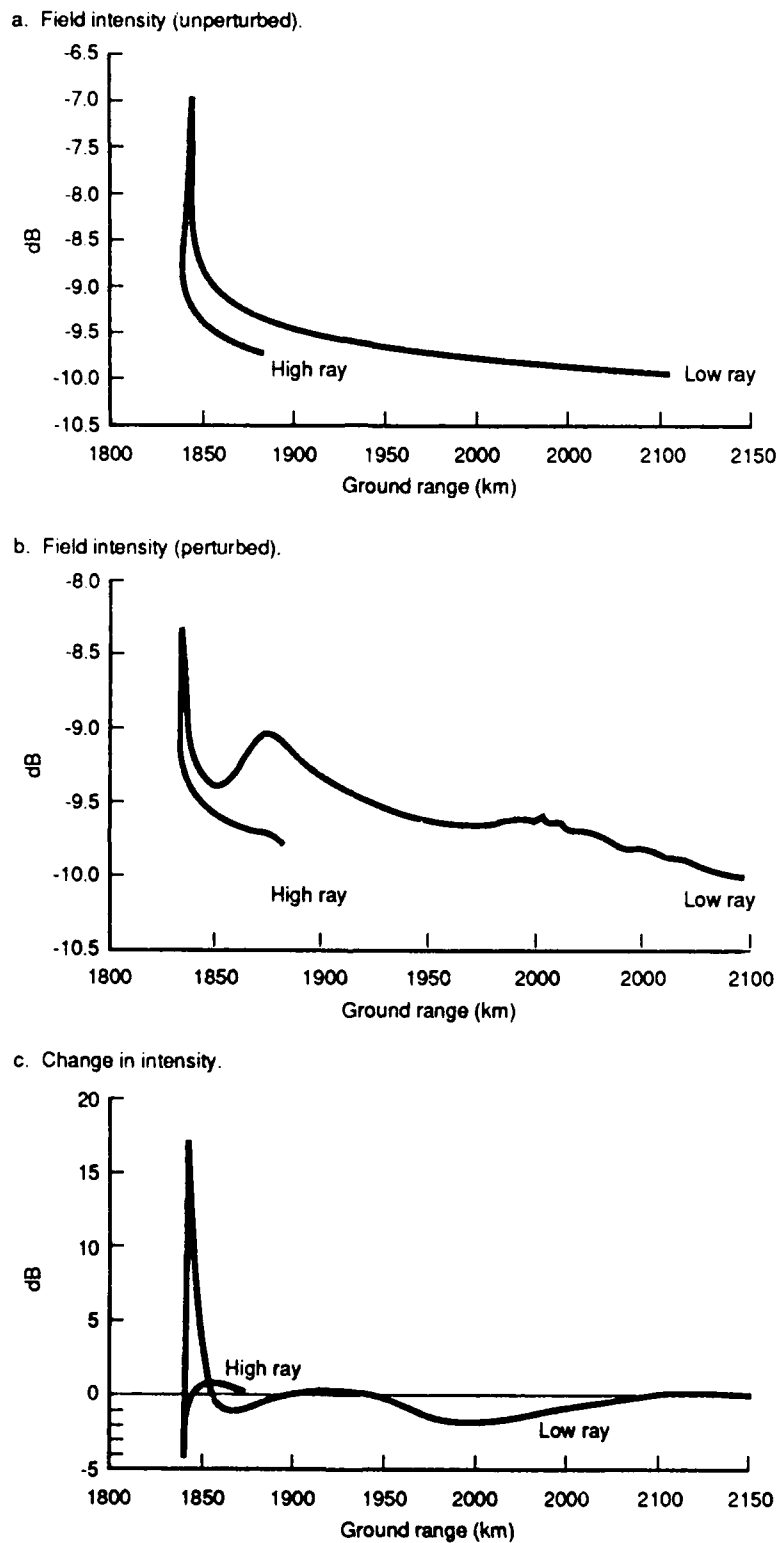


Figure 8. Steps in intensity change calculation, curtain antenna.

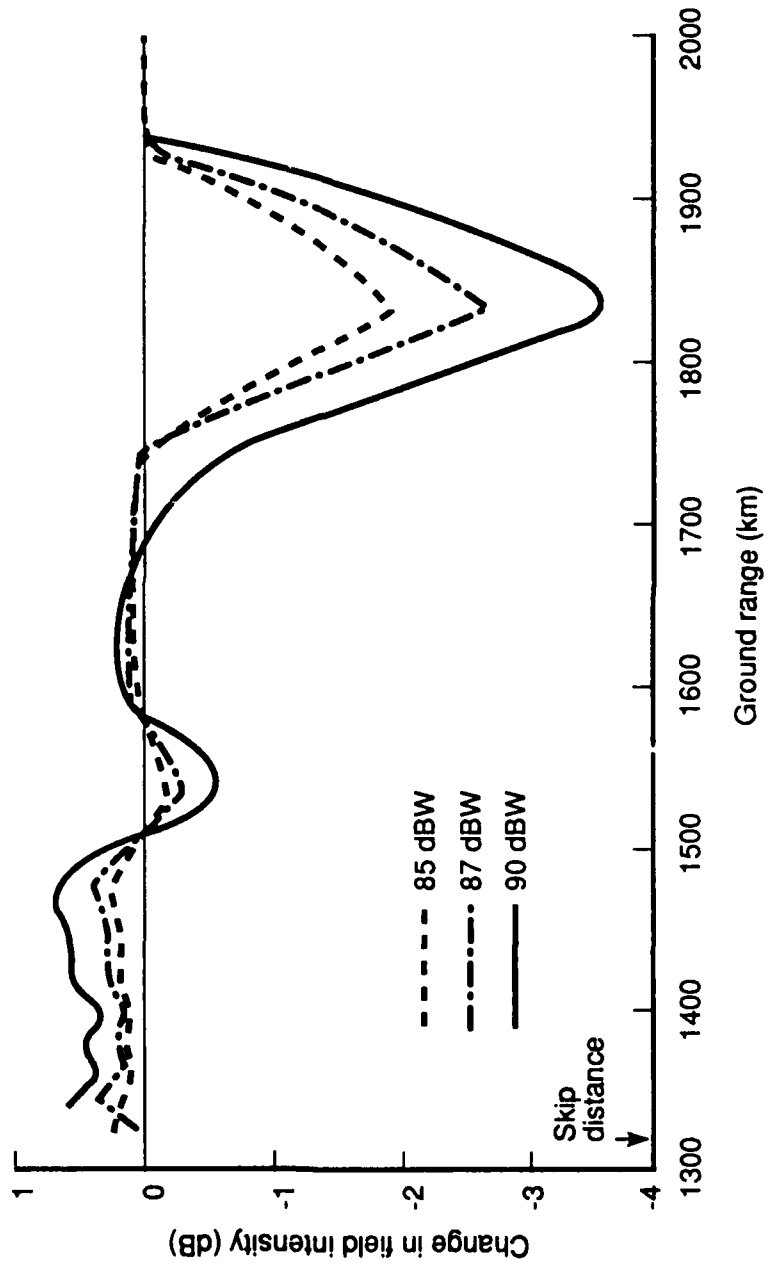


Figure 9a. Ground effect versus power-gain, Bochkarev model, 15 MHz, day, 60° dip.

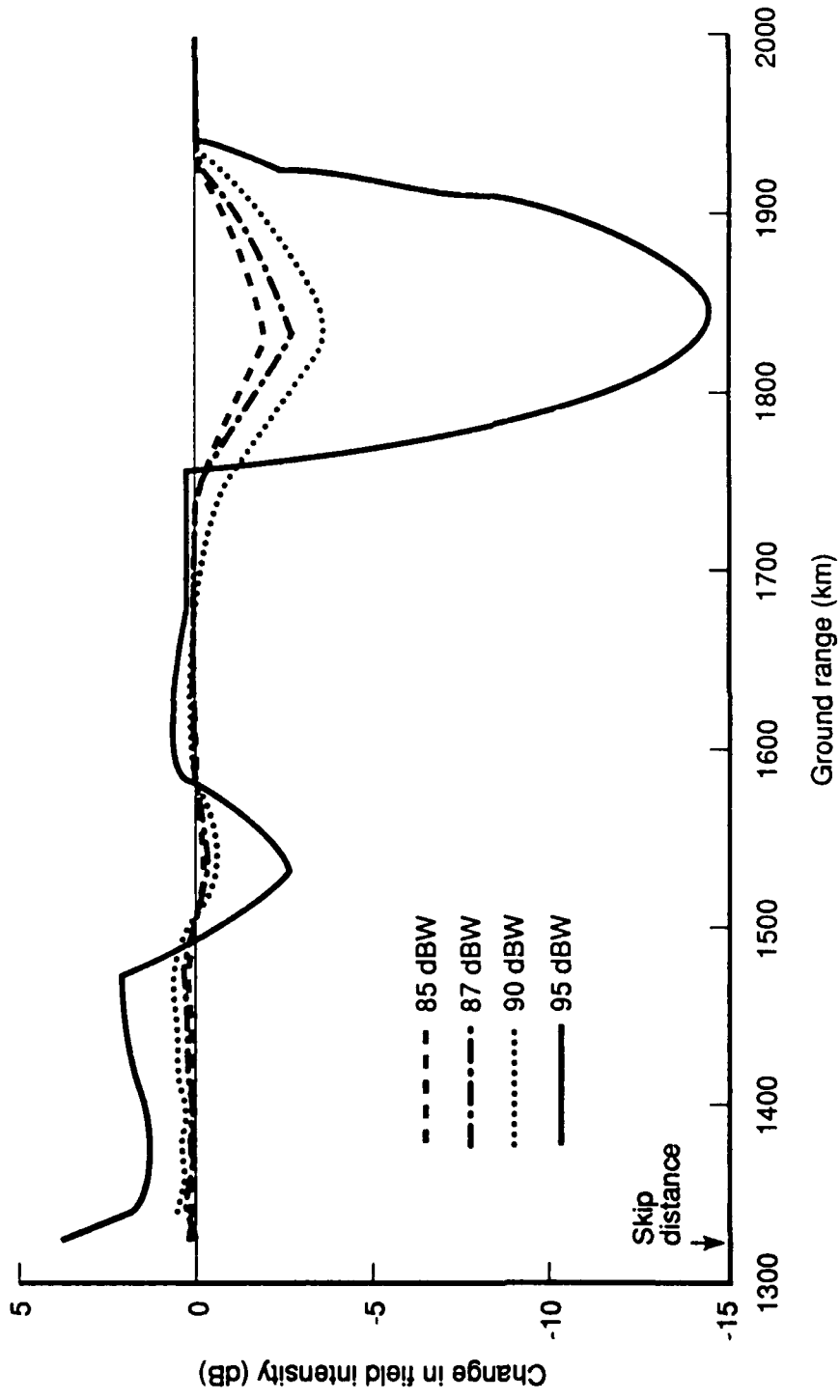


Figure 9b. Ground effect versus power-gain, Bochkarev model, 15 MHz, day, 60° dip. (Trend illustrating prediction of linear theory in nonlinear regime, 95 dbW.)

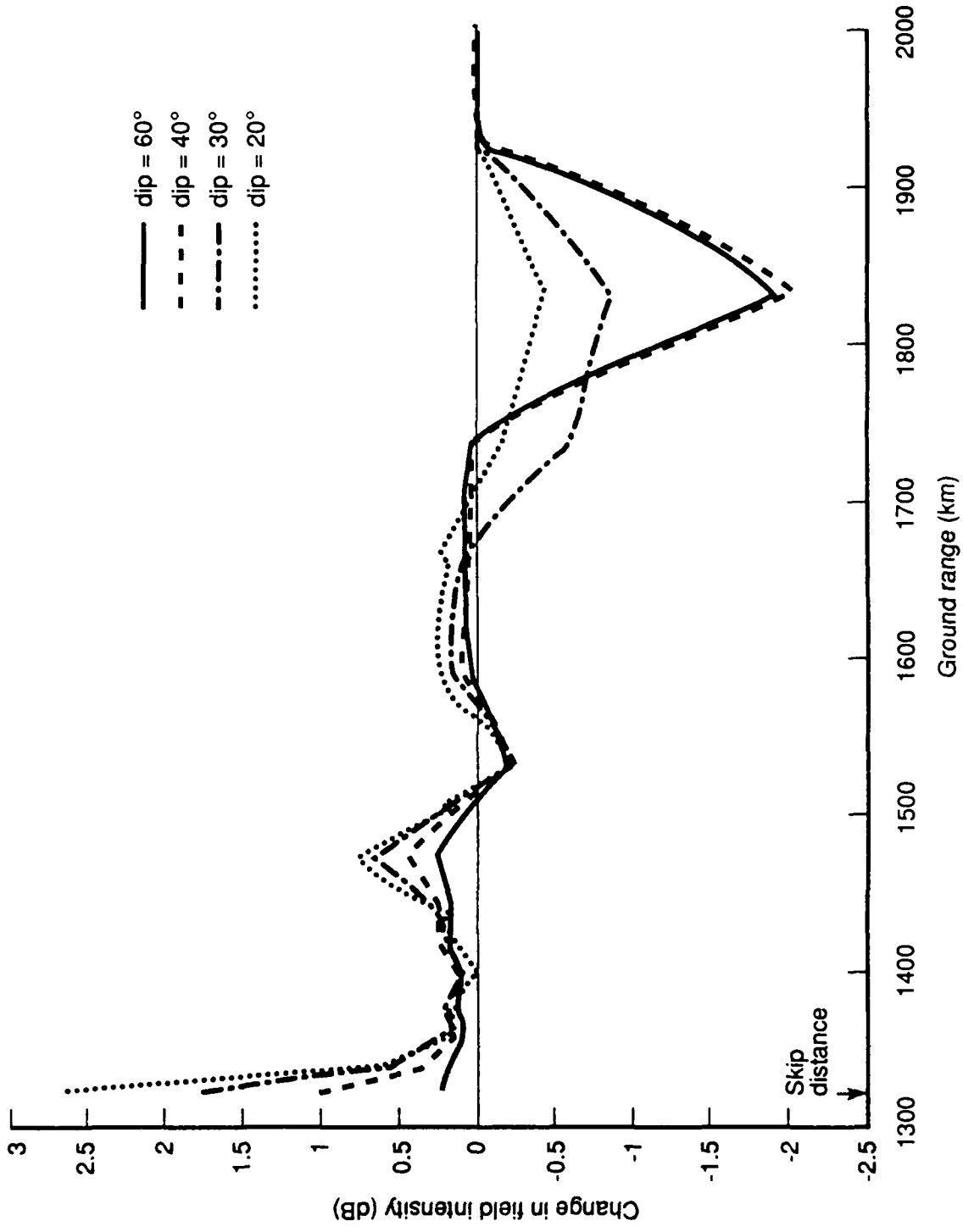


Figure 10. Ground effect versus dip angle, Bochkaev model, 15 MHz, day, 85 dBW.

tially perpendicular to the magnetic field (and are determined only by the azimuthal spread of the transmitter pattern). The maximum magnitude of  $n/N_0$  will therefore tend to increase. However, since the vertical dimension of the greatest perturbations will become small with decreasing dip angle, one must not assume that the ground effect will be monotonic in response. In fact, some complex relationship holds between the maximum magnitude of  $n/N_0$ , the size of the region over which the density change diffuses, and the signal change on the ground. This behavior is evident in the parametric study (Fig. 10). The ground effect near the interior skip increases with decreasing dip angle, but near the horizon it begins to decrease. There is also a competing trend in east-west propagation. As the field lines, and hence the diffusion direction, incline more toward the horizontal, rays will tend to refract at right angles to the east-west meridian. In our calculations, however, we have not allowed for ray refraction out of the plane of propagation; we have taken the perturbed region to be cylindrically symmetric.

Lastly, Figs. 11 and 12 show how the effect of the perturbation on ray arrival-angle varies with the power-gain product and the local magnetic dip angle, respectively. In the first case, we have fixed the dip angle at  $60^\circ$  and varied the power-gain product; in the second, the power-gain is fixed at 85 dBW and the dip angle is varied. The examples indicate only a few minutes of a degree change in ray angle of arrival.

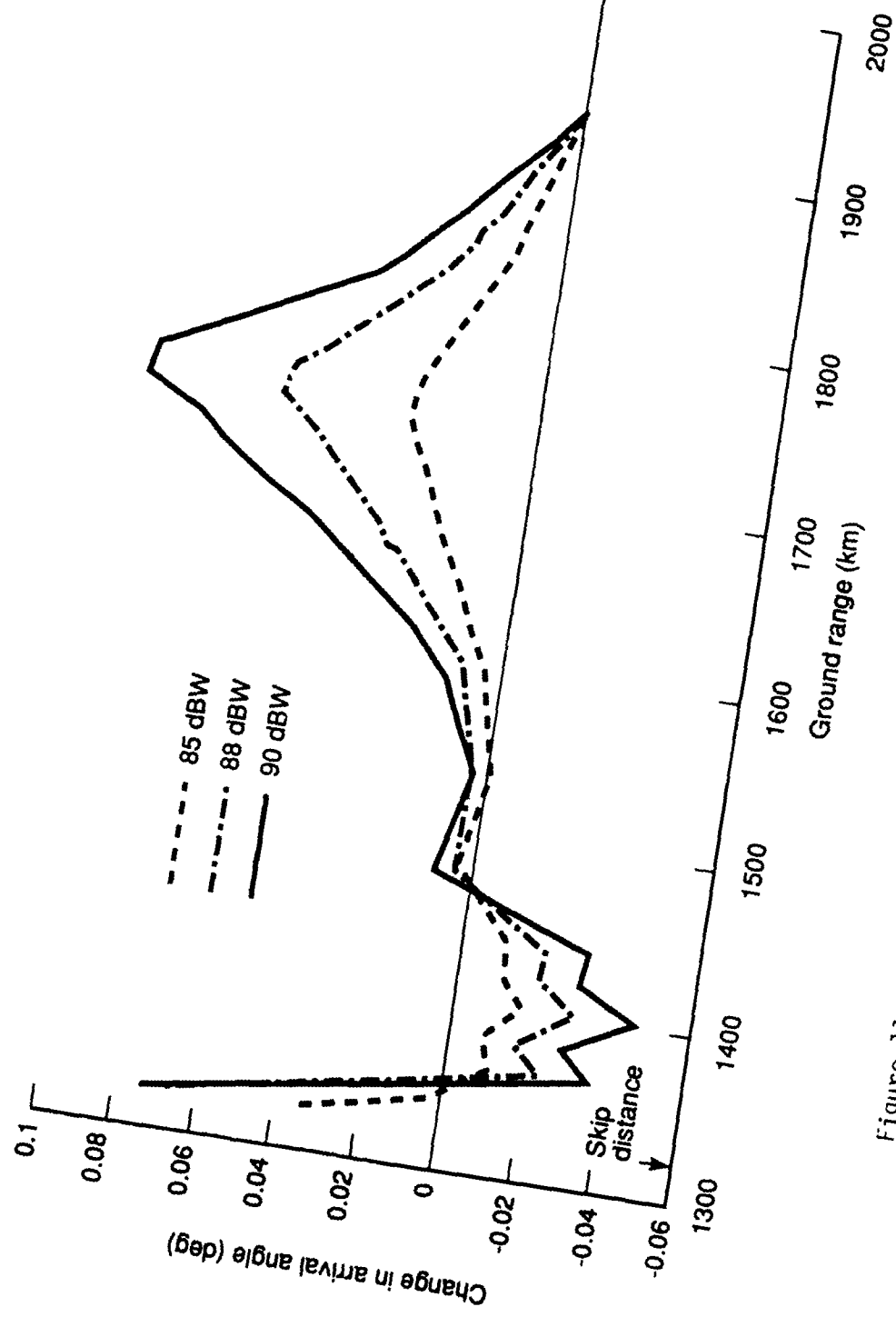


Figure 11. Change in arrival angle versus power gain, Bochkaev model, 15 MHz, day, 60° dip.

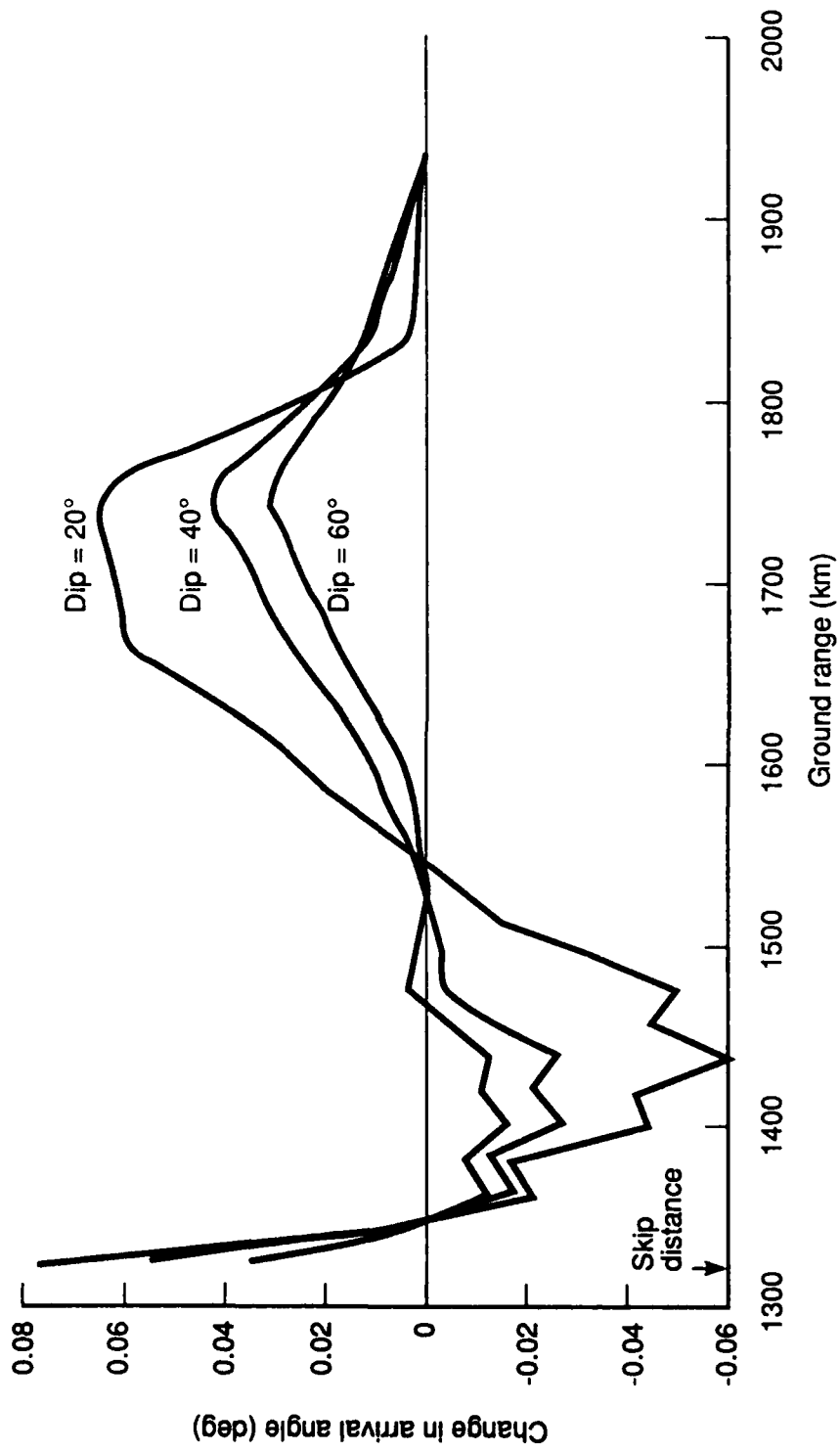


Figure 12. Change in arrival angle versus dip angle, Bochkarev model, 15 MHz, day, 85 dBW.

#### IV. CONCLUSIONS

Our calculations indicate ground-level field-strength changes of several dB might be produced by joule-heating of the ionosphere by intense oblique HF waves. Although small, these calculated field-strength changes are similar to the 3 dB change measured by Bochkarev and associates [1,2,3,4], who gave only sketchy details of their experimental parameters. Our calculated arrival-angle change of several arc minutes are much smaller than the 2 to 3 deg change reported by Bochkarev. Our results are extremely sensitive to the model ionosphere used and therefore indicate that an experiment should employ the widest possible range of frequencies and propagation conditions. An effective power of 90 dBW is far more likely to produce a detectable signal change than a power of 85 dBW. Our conclusions are based solely on joule-heating from linear waves, and omit plasma instabilities.

Our results pertain to steady-state effects. The time scale for these phenomena is roughly the characteristic diffusion time of the ionospheric layer in which strongest electric field focusing has occurred. This quantity,  $\tau_N$ , taken from Table 2, Vol. 1, is a function of the ambient recombination coefficient and plasma density (Eq. [19]). An experiment which took into account this waiting time might observe dipping and peaking of signal strength just past the skip distance (Figs. 7a through 7c). The difficulty of such measurements is that the diffusion "waiting time" is, in some cases, considerably longer ( $10^2 \sim 10^3$  s) than the average period of ambient ionospheric fluctuations.

## REFERENCES

1. Bochkarev, G. S., et al., "Effect of Artificial Perturbations of the Ionosphere on the Propagation of Short-Wave Signals," *Radiofizika*, Vol. 20, January 1979, pp. 158-160.
2. Bochkarev, G. S., et al., "Interaction of Decametric Radio Waves on Frequencies Close to the MUF of F2 During Oblique Propagation," *Geomagnet. Aeron.*, Vol. 19, No. 5, 1979, pp. 557-559.
3. Bochkarev, G. S., et al., "Nonlinear Interaction of Decametre Radio Waves at Close Frequencies in Oblique Propagation," *J. Atmos. Terr. Phys.*, Vol. 44, December 1982, pp. 1137-1141.
4. Bochkarev, G. S., et al., "Simulation of the Action of a Strong Obliquely Incident Wave on the Ionosphere," *Geomagnet. Aeron.*, Vol. 20, No. 5, 1980, pp. 592-595.
5. Field, E. C., R. M. Bloom, and K. E. Heikes, *Ionospheric Heating with Oblique Waves*, Vol. I. *Electron Density Perturbations*, Pacific-Sierra Research Corporation, Report 1864, September 1988, AFGL-TR-88-0336. **ADA216260**
6. Kershner, S. W., "High Performance Antenna Systems for New VOA Stations," *IEEE Trans. on Broadcasting*, Vol. 34, No. 2, June 1988.
7. Field, E. C., and C. R. Warber, *Ionospheric Modification with Obliquely Incident Radio Waves: Electron Heating and Parametric Instabilities*, Rome Air Development Center, Interim Report, RADC-TR-85-188, October 1985, ADA162603.
8. Field, E. C., and C. R. Warber, "Ionospheric Heating with Obliquely Incident Waves," *Geophys. Res. Letters*, Vol. 12, No. 11, November 1985, pp. 761-763.
9. Warren, R. E., R. N. DeWitt and C. R. Warber, "A Numerical Method for Extending Ray Trace Calculations of Radio Fields into Strong Focusing Regions," *Radio Sci.*, Vol. 17, May-June 1982, pp. 514-520.
10. Gurevich, A. V., *Nonlinear Phenomena in the Ionosphere*. Springer Verlag, New York City, 1978.
11. Jones, R. M., and J. J. Stephenson, *A Versatile Three-Dimensional Ray Tracing Computer Program for Radio Waves in the Ionosphere*. U.S. Department of Commerce, Washington, DC. OT Report 75-76, October 1975.

12. Nickisch, L. J., "Focusing in the Stationary Phase Approximation." *Radio Sci.*, Vol. 23, No. 2, March-April 1988, pp. 171-182.
13. Buckley, R., "On the Calculation of Intensity in Dispersive Inhomogenous Media in the Ray Approximation," *Proc. R. Soc. Lond.*, Vol. A 380, 1982, pp. 201-209.
14. Meltz, G., L. H. Holway, Jr., and N. M. Tomljanovich, "Ionospheric Heating by Powerful Radio Waves," *Radio Sci.*, Vol. 9, No. 11, November 1974, pp. 1049-1063.
15. Bernhardt, P. A., and L. M. Duncan, "The Feedback-Diffraction Theory of Ionospheric Heating," *J. of Atmos. and Terr. Phys.*, Vol. 44, No. 12, 1982, pp. 1061-1074.
16. Ratcliffe, J. A., *The Magneto-Ionic Theory and Its Applications to the Ionosphere. A Monograph*, University Press, Cambridge, Massachusetts 1959.